AD 667181

Reproduced by the
CLEARINGHOUSE
for Federal Scientific & Technical
Information Springfield Va. 22151

Distr
document

UNCLASSIFIED

AD 667 181

KINETICS OF NYLON AND PHENOLIC PYROLYSIS

H. E. Goldstein

Lockheed Missiles and Space Company
Sunnyvale, California

October 1965

Processed for . . .

DEFENSE DOCUMENTATION CENTER
DEFENSE SUPPLY AGENCY

CLEARINGHOUSE
FOR FEDERAL SCIENTIFIC AND TECHNICAL INFORMATION

U. S. DEPARTMENT OF COMMERCE / NATIONAL BUREAU OF STANDARDS / INSTITUTE FOR APPLIED TECHNOLOGY

Technical Report

KINETICS OF NYLON AND PHENOLIC PYROLYSIS

by
H. E. Goldstein

LMSC-667876 October 1965

Work Carried Out As Part of Lockheed Polaris
Advanced Materials Research Program

Distribution of this
document is unlimited

LOCKHEED MISSILES & SPACE COMPANY
A Group Division of Lockheed Aircraft Corporation
Sunnyvale, California

D D C
APR 5 1968

ABSTRACT

This report describes the pyrolysis kinetics of nylon 6-6 and phenolic CTL 91-LD, as derived from thermogravimetric analysis data (TGA). Individual rate equations and kinetic coefficients for the two polymers are presented and combined to yield a multi-step pyrolysis rate equation for composited nylon/phenolic.

The derived rate equations are verified by comparing them to thermogravimetric data taken at rates of sample temperature rise varying from 3° C/min to 100° C/min. Weight-loss data for the nylon/phenolic composite, during both isothermal pyrolysis and pyrolysis at programmed rates of temperature rise, are accurately correlated by the multi-step pyrolysis rate equation.

This report was prepared by the Materials Group of the Launch and Entry Thermodynamics Department, Flight Technology Division. The work itself, part of the Lockheed Polaris Advanced Materials Program, was completed in October 1963.

ACKNOWLEDGMENTS

The author gratefully acknowledges the contributions to this work of M. Honma and R. Whethern who provided TGA data for the analysis, to G. Steinbach who performed most of the computational work, including programming of the exponential integral $E_2(X)$, and to P. Schneider for editorial assistance in preparing the report.

CONTENTS

Section		Page
	ABSTRACT	ii
	ACKNOWLEDGMENTS	iii
	ILLUSTRATIONS AND TABLE	v
	NOTATION	vi
1	INTRODUCTION	1
2	MEASUREMENT METHODS	2
3	THEORY AND ANALYSIS	5
4	CORRELATION OF EXPERIMENTAL DATA AND THEORY	23
5	CONCLUSIONS	37
6	REFERENCES	37
	APPENDIX	38

ILLUSTRATIONS

Figure		Page
1	Thermogravimetric Analysis Apparatus	3
2	TGA Rate Data – Phenolic 91LD Resin (3°C/min)	7
3	TGA Rate Data – Phenolic 91LD Resin (18°C/min)	8
4	TGA Rate Data – Nylon 6-6 Fabric (3°C/min)	9
5	TGA Rate Data – Nylon 6-6 Fabric (18°C/min)	10
6	TGA Rate Data – 1:1 Resin-Fabric Weight Ratio Composite (3°C/min)	11
7	Derivative TGA Plot -- Phenolic 91-LD Resin (3°C/min)	12
8	Derivative TGA Plot – Nylon 6-6 Fabric (3°C/min)	13
9	Second Derivative Plot [Eq. (17)] Used to Determine Reaction Order and Activation Energy	17
10	Rate Equation Ratio Plot [Eq. (20)] Used to Determine Reaction Order	19
11	Arrhenius Correlation of TGA Rate Data	20
12	Comparison of Theory and TGA Rate Data – Phenolic 91-LD Resin	26
13	Comparison of Theory and TGA Rate Data – Nylon 6-6 Fabric	27
14	Comparison of Theory and TGA Rate Data – 1:1 Resin-Fabric Weight Ratio Composite (Isothermal)	29
15	Comparison of Theory and TGA Rate Data – 1:1 Resin-Fabric Weight Ratio Composite (3°C/min)	31
16	Comparison of Theory and TGA Rate Data – 1:1 Resin-Fabric Weight Ratio Composite (18°C/min)	32
17	Comparison of Theory and TGA Rate Data – 1:1 Resin-Fabric Weight Ratio Composite (60°C/min)	33
18	Comparison of Theory and TGA Rate Data – General Electric Nylon-Phenolic (18°C/min)	35
19	Comparison of Theory and TGA Rate Data – General Electric Nylon-Phenolic (3°C/min)	36

TABLE

Table		
A-1	The Exponential Integral	39

NOTATION

E	Arrhenius activation energy (Btu/lb-mole)
k_f	Arrhenius rate coefficient (sec^{-1})
k_o	specific reaction constant (sec^{-1})
n	reaction order
R	universal gas constant [Btu/lb-mole (°R)]
TGA	thermogravimetric analysis
w	weight
θ	time
Γ	weight fraction of nylon-phenolic composite

Subscripts

a, b	denoting different rates of temperature rise
c	char
comp	composite
g	gas
N	nylon
o	initial condition
P	phenolic
pyr	pyrolysis
S	solid plastic
I, II	phenolic reactions I and II respectively

Section 1
INTRODUCTION

The simultaneous depolymerization of a composite containing a thermosetting resin and a thermoplastic fiber is difficult to formulate analytically. When heated, each polymer depolymerizes by a characteristic kinetic process in converting the condensed phase to solid and gaseous products. Detailed thermochemical and kinetic analyses of a decomposing plastic require that the time-temperature course of the weight-loss process be accurately described in a general manner.

In previous studies, pyrolysis of nylon, phenolic, and their composites has been characterized by single-step kinetic processes (Refs. 1, 2, and 3). Agreement between the single-step kinetic theory and TGA data for phenolic and for nylon-phenolic composites is less than satisfactory, and the validity of extrapolating this theory to conditions far removed from laboratory conditions is questionable. For these reasons, a detailed kinetic study of nylon, phenolic, and a 1:1 weight-ratio nylon-phenolic composite was undertaken. The purpose of this study was to derive a rate equation and appropriate kinetic coefficients for use in solution of the transient thermal-response problem for nylon-phenolic composites. The particular constitutents considered were nylon 6-6 fabric and 91-LD phenolic resin.

Section 2
MEASUREMENT METHODS

Following is a description of the instrument and procedures used by LMSC (Ref. 4) to obtain TGA data for the kinetics analysis.

An American Instrument Company thermograv was used for the thermogravimetric measurements. A schematic diagram of the instrument is shown in Fig. 1. The weight lost (or gained) by the sample moves the armature in or out of the transducer's magnetic field causing changes in the field strength which, after suitable amplification and modulation, is registered on the Y axis of the recorder. The sample thermocouple, located in the well adjacent to the sample, provides a continuous reading of material temperature. A timing device, electromechanically connecting heater and recorder, indicates time marks at 1, 5, and 20 min intervals. The furnace can be programmed to give sample temperature rates of 3, 6, 9, 12, 15, and 18°C per min, with a maximum rate of about 25°C per min. The temperature range is from 0 to 1000°C with selective ranges within this limit (for example, 0° −500°C, 200° −500°C, etc.). There is a variable time scale with intervals from 0−50, 0−100, 0−200, and 0−400 minutes for isothermal experiments. Measurements can be performed in various atmospheres or in vacuum.

Operational procedure was as follows: A sample (250 mg) was prepared in block form and placed in the center of the sample holder. After assembling sample holder, rod support, and spring, the zero point was adjusted by addition of tare weights, and the recorder pen was set to proper temperature position on the graph. The quartz well was then centered about the sample holder and clamped into position. A selected gas flow was established and the temperature program adjusted for a preselected rise rate and end point. After several minutes of flushing with gas, the recorder was readjusted electronically for the difference between air and gas buoyancy. During initial temperature rise, the gain control of the recorder was adjusted to compensate for

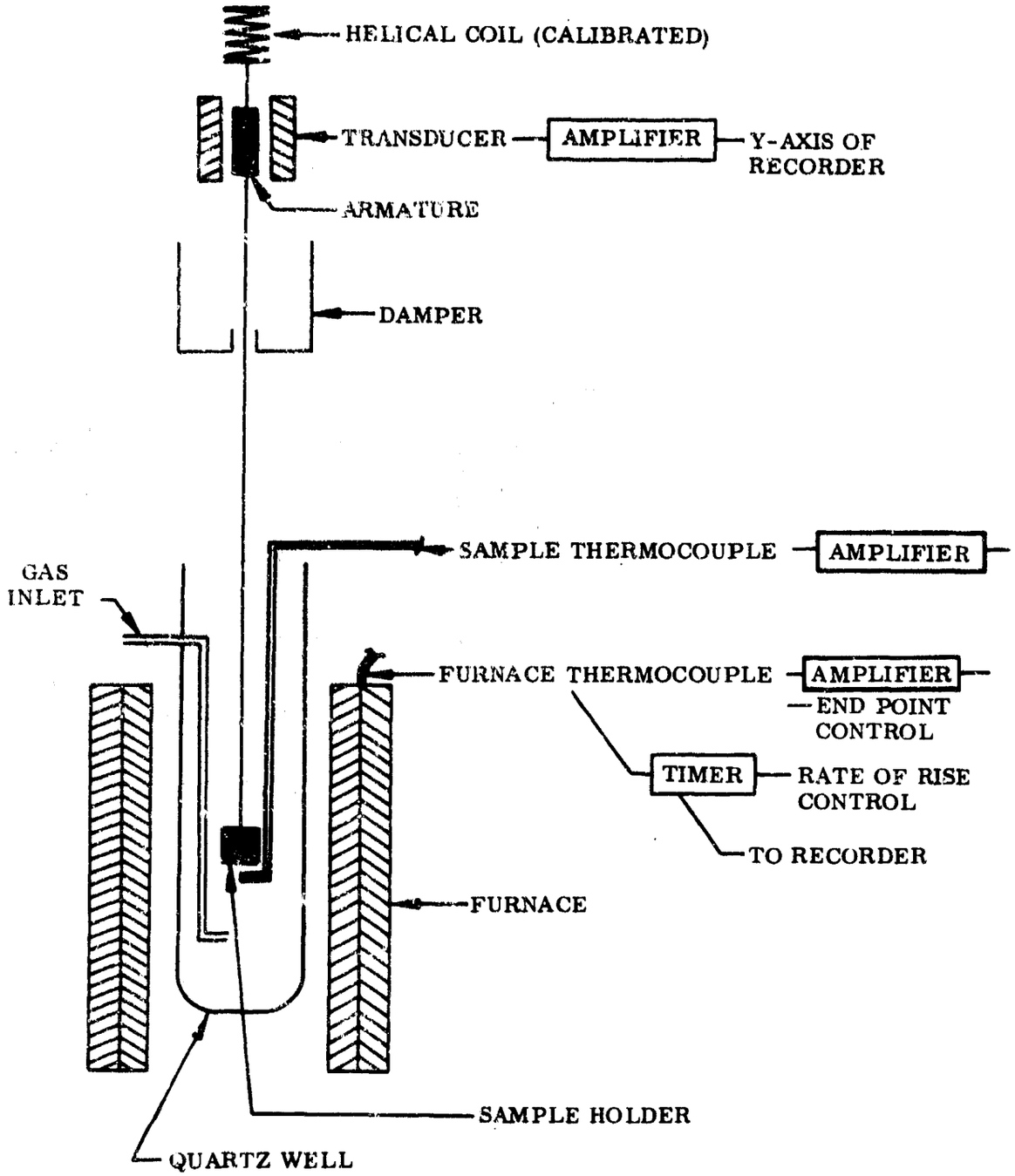

Fig. 1 Thermogravimetric Analysis Apparatus

temperature-induced fluctuations. After the preset temperature was reached the instrument was shut off, allowed to cool, and the residue weighed to check recorder weight-loss readings (method of Ref. 4).

Section 3
THEORY AND ANALYSIS

The pyrolysis of a material to char and gases may be described by the following reaction scheme:

$$w_o \rightarrow w_g + w_c \tag{1}$$

For an irreversible reaction the rate of disappearance of w_o is given by

$$-\frac{d(w/w_o)}{d\theta} = k_f\, f\left(\frac{w - w_c}{w_o}\right) \tag{2}$$

with the following definitions:

$$f\left(\frac{w - w_c}{w_o}\right) = \left(\frac{w - w_c}{w_o}\right)^n \tag{3}$$

$$k_f = k_o\, e^{-E/RT} \tag{4}$$

Here

w = weight of condensed material
w_o = initial weight of condensed material
w_c = weight of condensed material retained as char
θ = time
k_f = Arrhenius rate coefficient (sec^{-1})
k_o = specific reaction constant (sec^{-1})
E = Arrhenius activation energy (Btu/lb-mole)
R = universal gas constant [Btu/lb-mole (°R)]
n = reaction order

The final rate equation then takes the form

$$\frac{d(w/w_o)}{d\theta} = - k_o e^{-E/RT} \left(\frac{w - w_c}{w_o}\right)^n \tag{5}$$

Thermogravimetric analysis (TGA) gives the weight of material pyrolyzed versus temperature for a pyrolysis carried out at a fixed rate of sample temperature rise. Thus

$$\frac{dT}{d\theta} = C \tag{6}$$

Substituting Eq. (6) into Eq. (5) gives

$$\frac{d(w/w_o)}{dT} = - \frac{k_o}{C} e^{-E/RT} \left(\frac{w - w_c}{w_o}\right)^n \tag{7}$$

TGA data for nylon and phenolic at $C = 3$ and 18°C per min are shown in Figs. 2, 3, 4, and 5. Figure 6 shows a TGA run for the nylon-phenolic composite at $C = 3$°C per min. From data in Figs. 2 through 5, the rate of weight loss with respect to temperature was determined for each material. Figures 7 and 8 are plots of temperature rate of weight loss (normalized to initial sample weight) versus temperature for phenolic and nylon respectively.

Figure 7 shows two maximums in rate of weight loss for phenolic, indicating that pyrolysis of the phenolic takes place in two major reactions. The rate equation for the two-step phenolic reaction takes the form

$$\left[\frac{d(w/w_o)}{dT}\right]_P = \left[\frac{d(w_I/w_o)}{dT}\right]_I + \left[\frac{d(w_{II}/w_o)}{dT}\right]_{II} \tag{8}$$

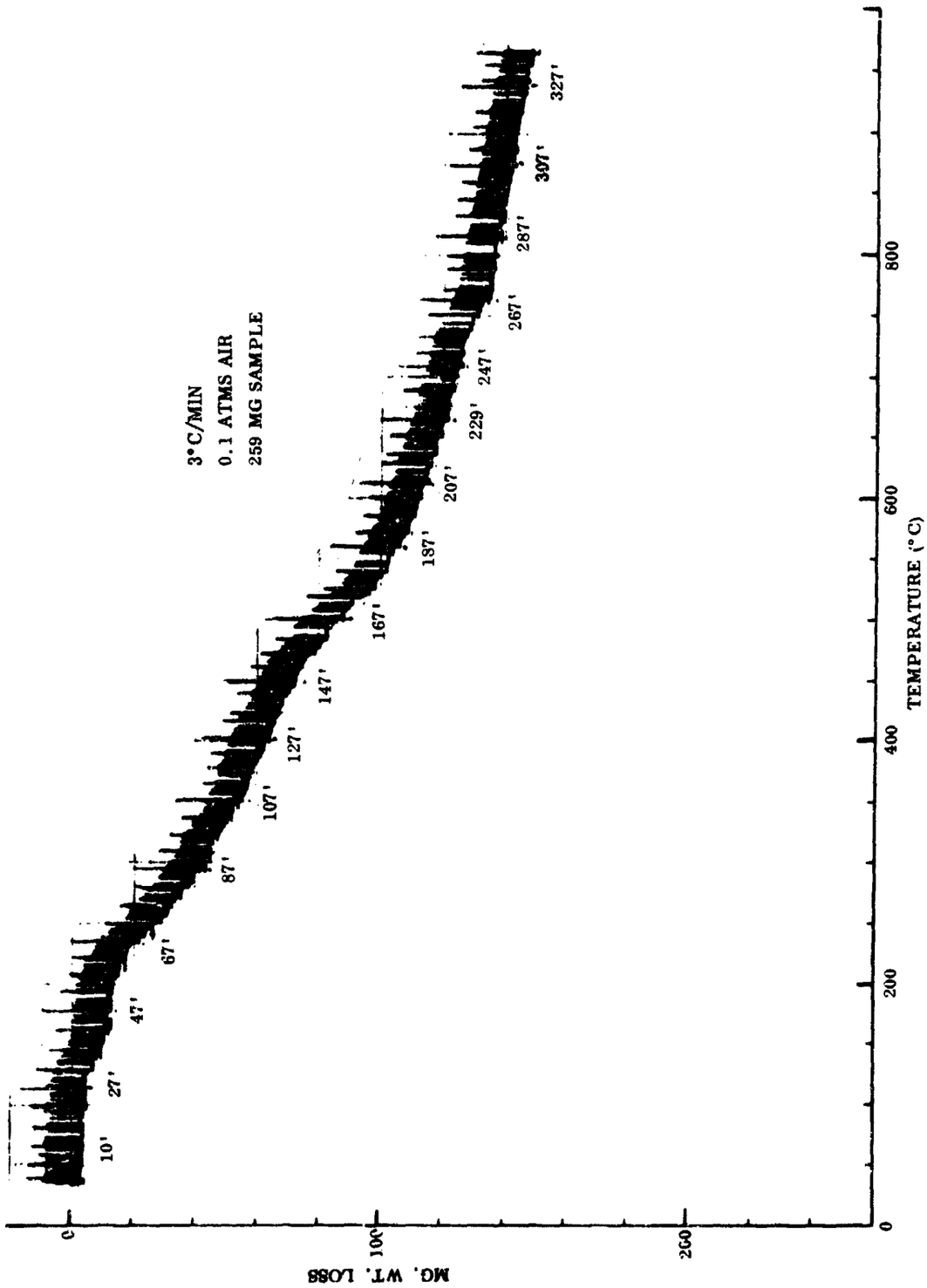

Fig. 2 TGA Rate Data – Phenolic 91LD Resin

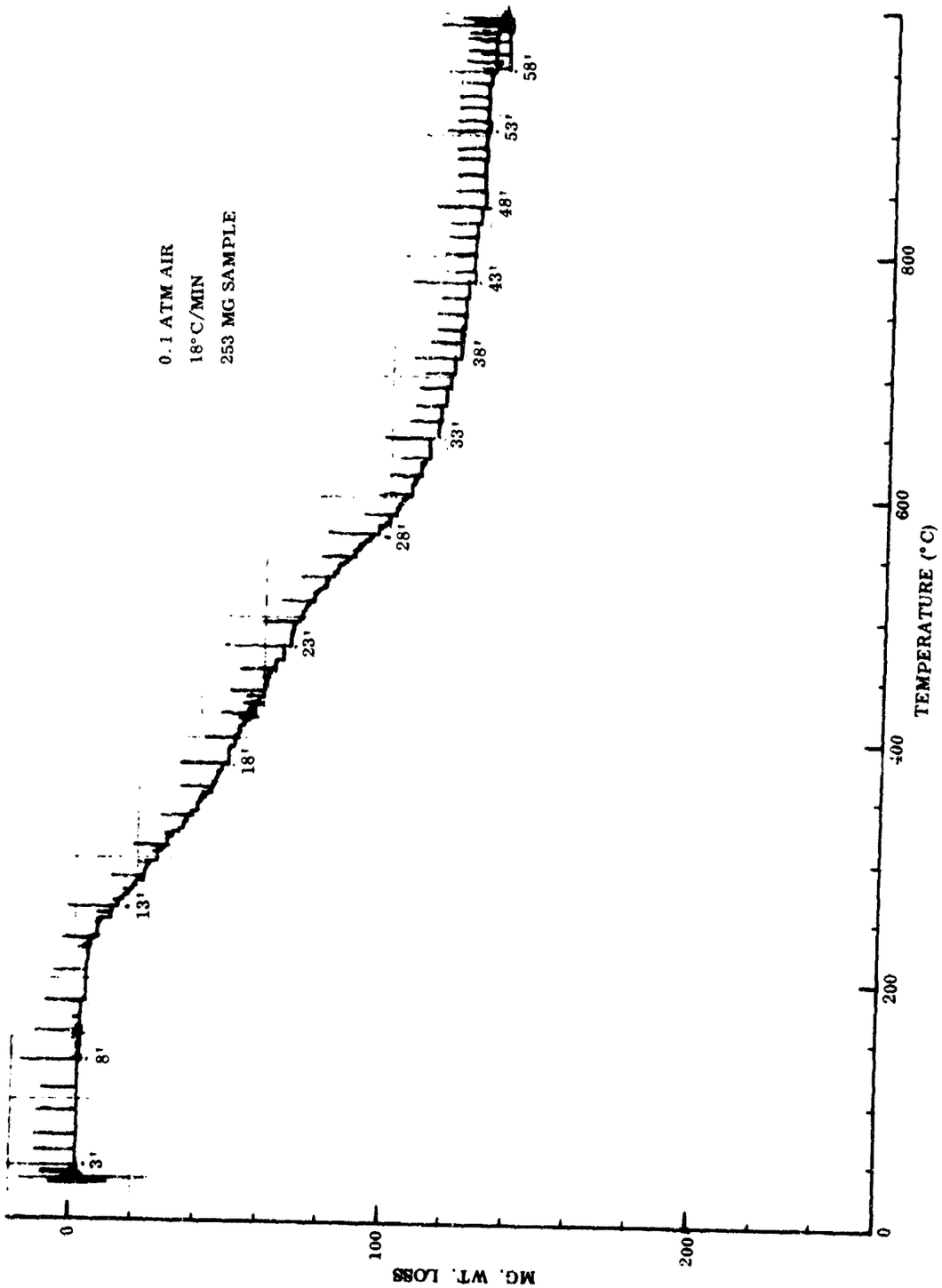

Fig. 3 TGA Rate Data – Phenolic 91LD Resin

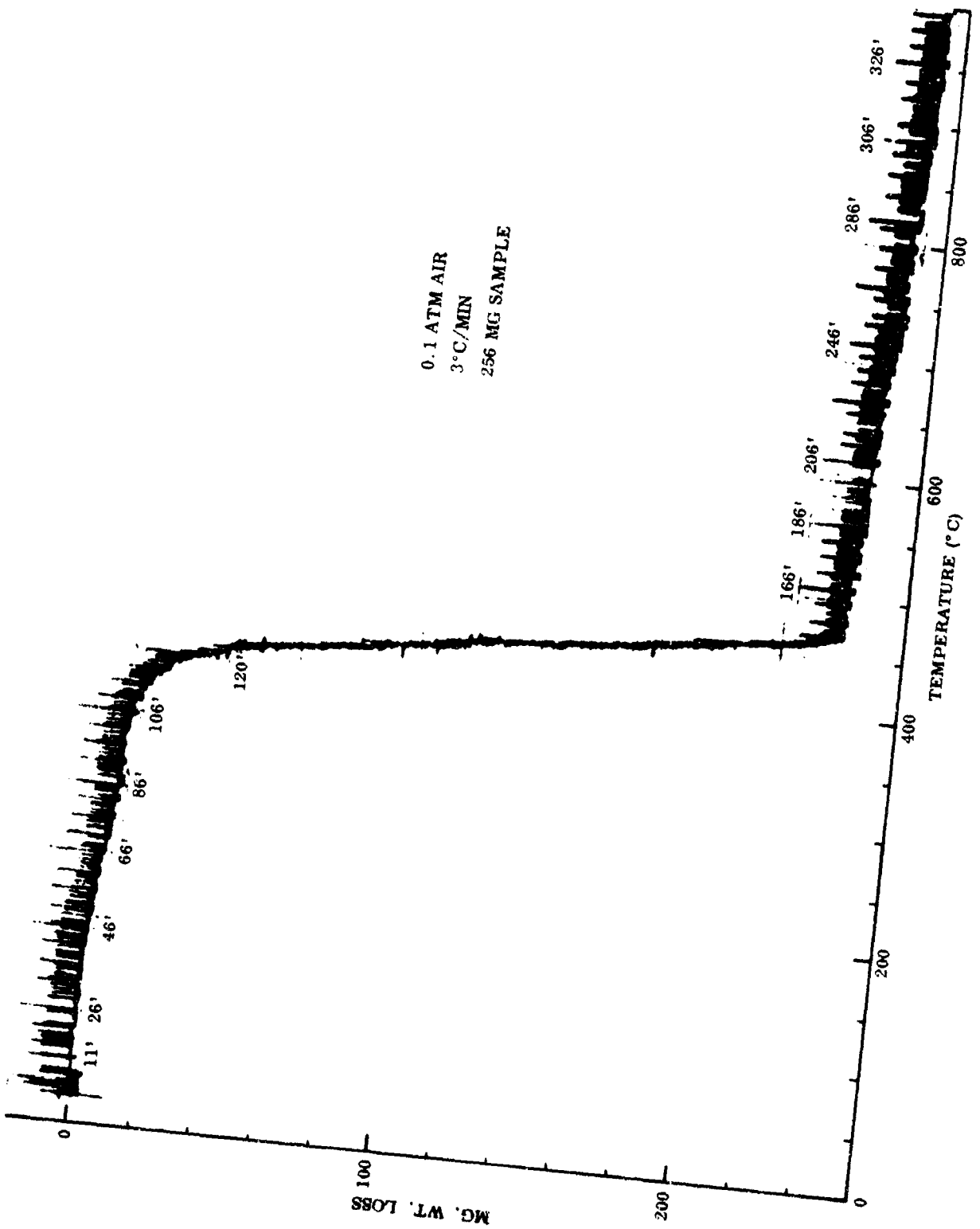

Fig. 4 TGA Rate Data – Nylon 6-6 Fabric

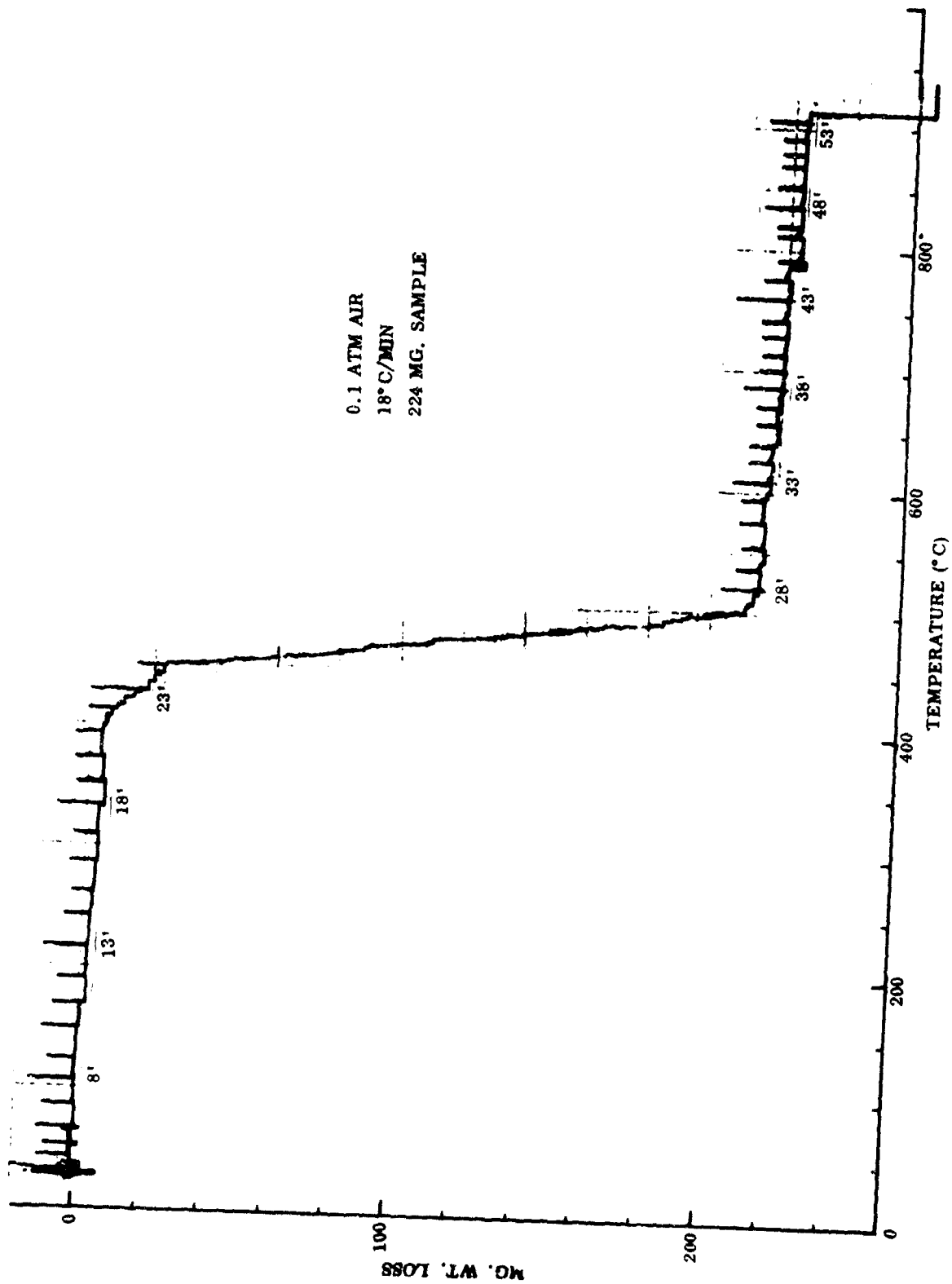

Fig. 5 TGA Rate Data – Nylon 6-6 Fabric

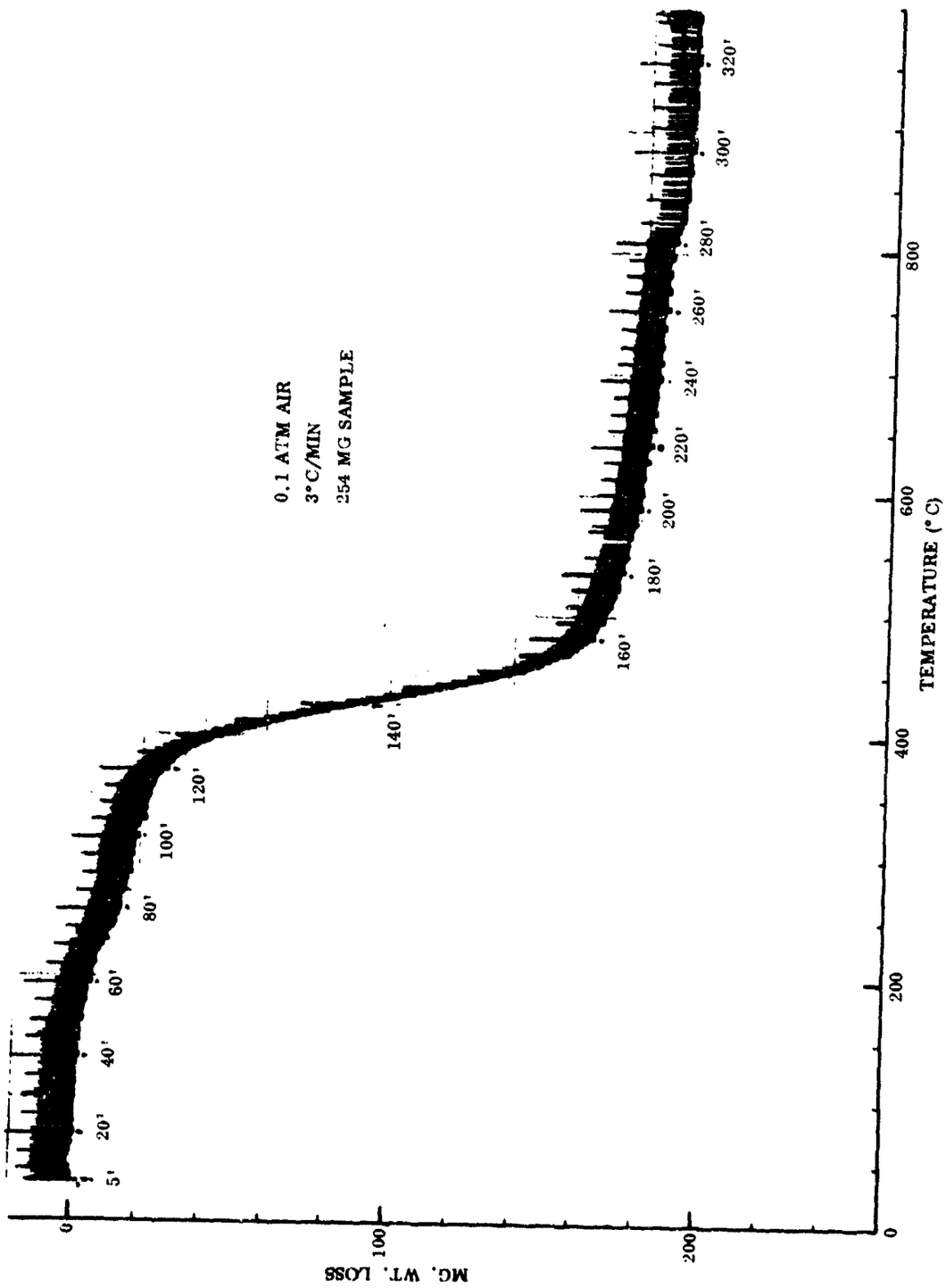

Fig. 6 TGA Rate Data – 1:1 Resin-Fabric Weight Ratio Composite

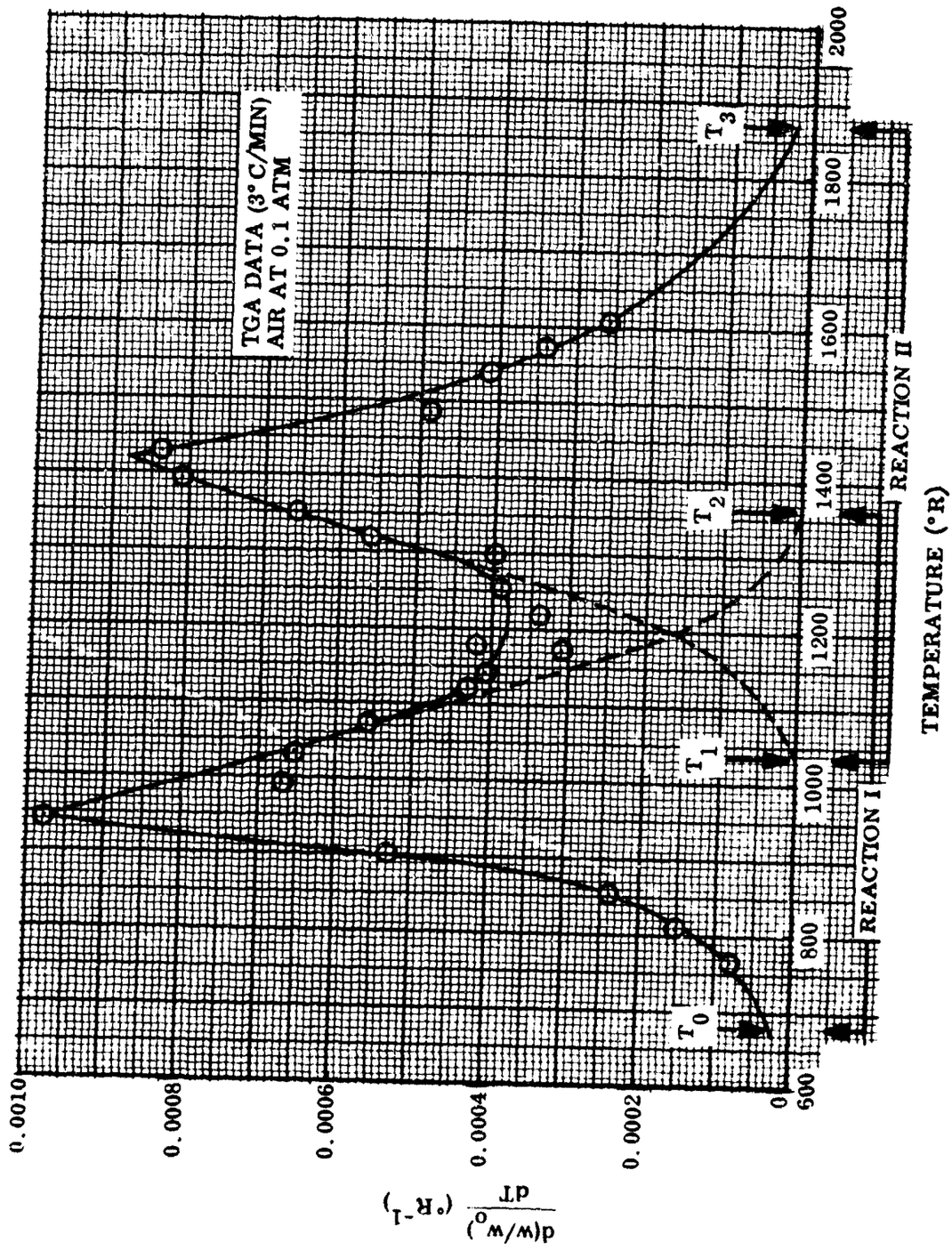

Fig. 7 Derivative TGA Plot – Phenolic 91LD Resin

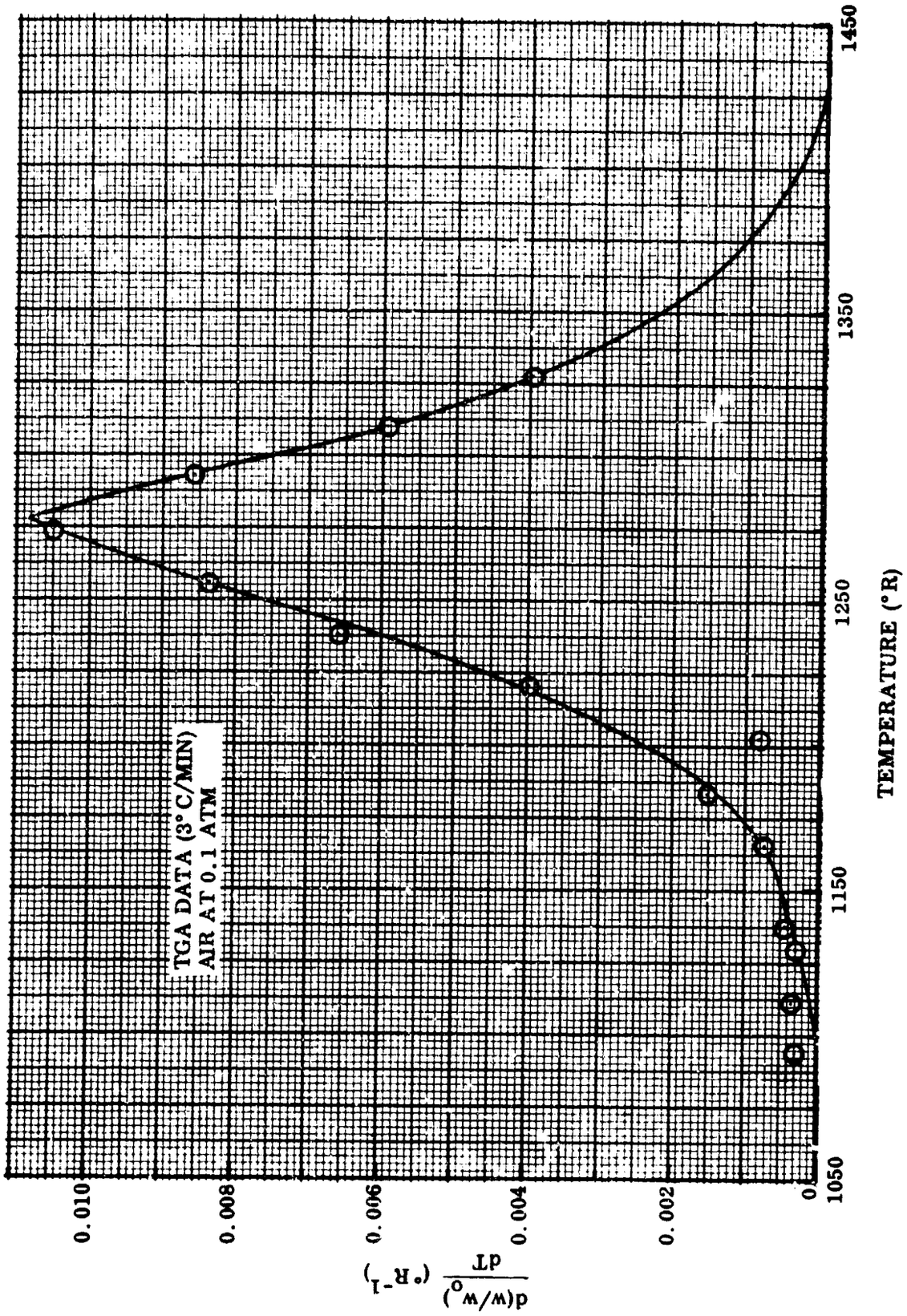

Fig. 8 Derivative TGA Plot – Nylon 6-6 Fabric

Rate equations for reactions I and II are both assumed to be defined by Eq. (5). Then Eq. (8) becomes

$$\frac{d(w/w_o)}{dT} = -\left[\frac{k_{oI}}{C} e^{-E_I/RT}\left(\frac{w_I - w_{cI}}{w_{oI}}\right)^{n_I} + \frac{k_{oII}}{C} e^{-E_{II}/RT}\left(\frac{w_{II} - w_{cII}}{w_{oII}}\right)^{n_{II}}\right] \tag{9}$$

For Eq. (9) to be true, the following identities must hold:

$$\frac{w}{w_o} = \frac{w_I}{w_o} + \frac{w_{II}}{w_o} \tag{10}$$

$$1 = \frac{w_{oI}}{w_o} + \frac{w_{oII}}{w_o} \tag{11}$$

The weight fractions w_{oI}/w_o and w_{oII}/w_o are weight fractions of the virgin plastic taking part in each reaction; similarly w_{cI}/w_o and w_{cII}/w_o are the weight fractions of reacting virgin plastic remaining in the solid state at completion of each reaction. When reaction I has gone to completion, the weight pyrolyzed will be the initial weight considered in the reaction w_{oI} less the weight of partially reacted solid w_{cI}. By extrapolating the data for reaction I in Fig. 7 to zero at T_2, and graphically integrating from T_o to T_2, the weight fraction pyrolyzed can be obtained as

$$\frac{w_{oI} - w_{cI}}{w_o} = \int_{T_o}^{T_2} \frac{d(w/w_o)}{dT} dT = \frac{\Delta w}{w_o} = 0.25 \tag{12}$$

The corresponding calculation for reaction II (using Fig. 7) is

$$\frac{w_{oII} - w_{cII}}{w_o} = \int_{T_1}^{T_3} \frac{d(w/w_o)}{dT} dT = \frac{\Delta w}{w_o} = 0.25 \tag{13}$$

Based on TGA and high-temperature pyrolysis data, the char weight-fraction adopted is 0.50. Then from Eqs. (11), (12), and (13) the following values are obtained:

$$\frac{w_{oII}}{w_o} = 0.25 + 0.5 = 0.75$$

$$\frac{w_{oI}}{w_o} = 1 - 0.75 = 0.25$$

$$\frac{w_{cI}}{w_o} = 0.25 - 0.25 = 0$$

The kinetic coefficients E, k_o, and n, are determined for each reaction. These parameters can be found using the following three correlation methods:

Method 1 is that of Freeman and Carrol (Ref. 5); it gives both the activation energy E and reaction order n. Taking logarithms of Eq. (7)

$$\text{Log}\left[-\frac{d(w/w_o)}{dT}\right] = \log\frac{k_o}{C} - \left(\frac{E}{RT}\right)\log e + n\log\left(\frac{w - w_c}{w_o}\right) \tag{14}$$

and finite differences of Eq. (14), gives

$$\Delta\,\text{Log}\left[-\frac{d(w/w_o)}{dT}\right] = \Delta\log\frac{k_o}{C} - \Delta\left(\frac{E}{RT}\right)\log e + n\,\Delta\log\left(\frac{w - w_c}{w_o}\right) \tag{15}$$

For constant C and k_o

$$\Delta\log\frac{k_o}{C} = 0 \tag{16}$$

Combining Eqs. (15) and (16) and assuming E and n constant

$$\frac{\Delta \log [-d(w/w_o)/dT]}{\Delta \log [(w - w_c)/w_o]} = -\frac{E}{R}\left\{\frac{\Delta (1/T)}{\Delta \log [(w - w_c)/w_o]}\right\}\log e + n \qquad (17)$$

A plot of the left side of Eq. (17) versus the bracketed term on the right side gives $-(E/R) \log e$ as slope and n as the intercept. Plots of this equation for the two phenolic reactions are shown in Fig. 9.

Method 2 gives the reaction order n independently. For a pyrolysis reaction carried out at two rates of temperature rise C_a and C_b, Eq. (7) may be evaluated for each rate of temperature rise. As in the first method, activation energy E, specific rate constant k_o, and reaction order n are assumed constant. A ratio of Eq. (7) evaluated for C_a to Eq. (7) evaluated for C_b is then

$$\left\{\frac{[d (w/w_o)/dT]_a}{[d (w/w_o)/dT]_b}\right\} = \frac{k_o \exp(-E/RT_a)\, [(w - w_c)/w_o]_a^n / c_a}{k_o \exp(-E/RT)\, [(w - w_c)/w_o]_b^n / c_b} \qquad (18)$$

For $T_a = T_b$

$$\left\{\frac{[d (w/w_o)/dT]_a^{c_a}}{[d (w/w_o)/dT]_b^{c_b}}\right\} = \left\{\frac{[(w - w_c)/w_o]_a}{[(w - w_c)/w_o]_b}\right\}^n \qquad (19)$$

Taking logarithms of each side of Eq. (19) and substituting Eq. (6) gives

$$\log \left\{\frac{[d (w/w_o)/d\theta]_a}{[d (w/w_o)/d\theta]_b}\right\} = n \log \left\{\frac{[(w - w_c)/w_o]_a}{[(w - w_c)/w_o]_b}\right\} \qquad (20)$$

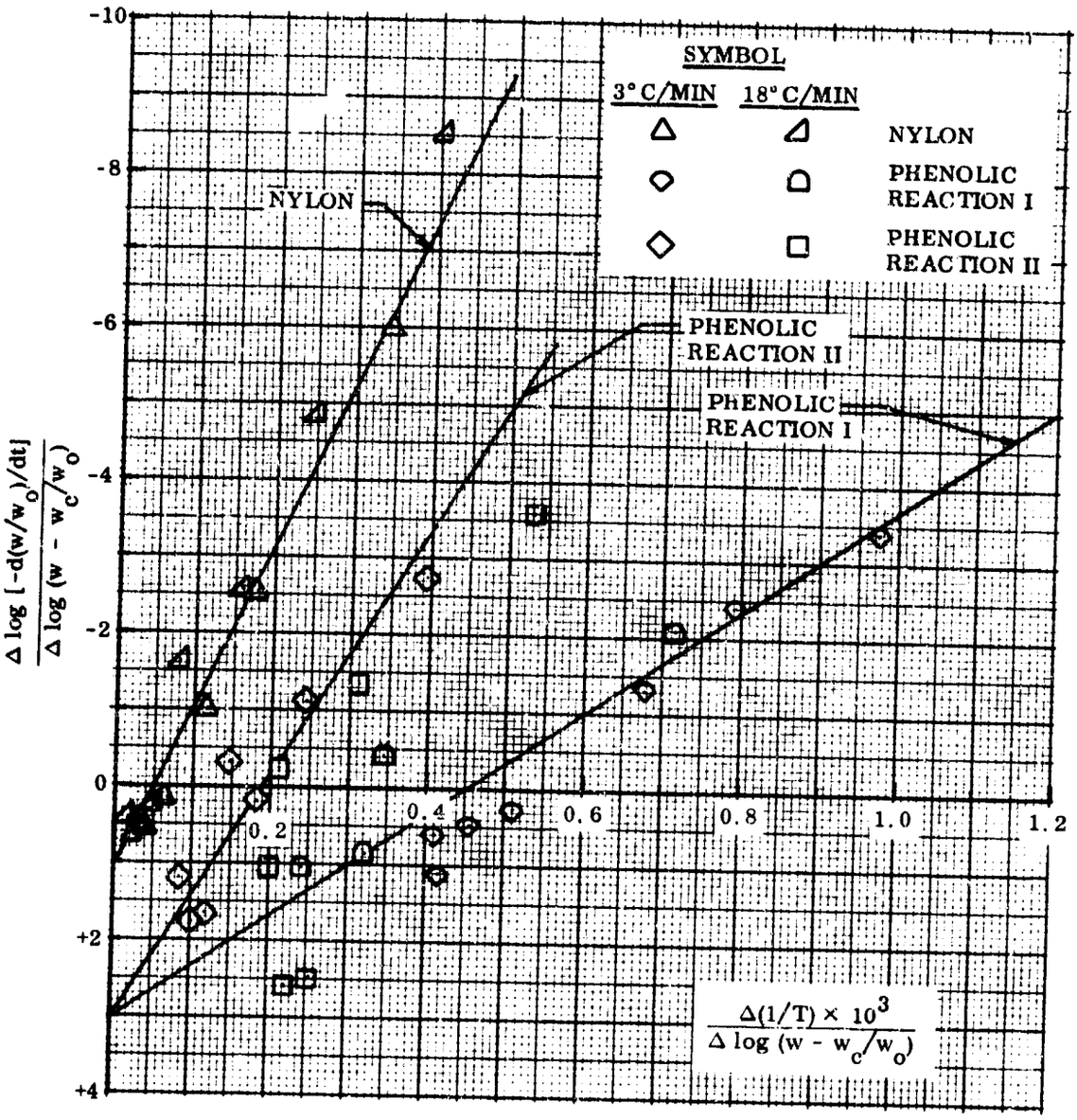

Fig. 9 Second Derivative Plot, Eq. (17), Used to Determine Reaction Order and Activation Energy

Equation (20) describes a straight line with intercept zero and slope n. Since the intercept is a constant, a line may be determined for every value of n. Figure 10 shows plots of these lines for n = 0.5, 1, 2, 3, 4, and 5. Data points for phenolic, calculated from Figs. 1 and 2, are also plotted.

Method 3 is based on the Arrhenius relation. Equation (7) can be rearranged as

$$k_o e^{-E/RT} = - \frac{d(w/w_o)}{dT} \left(\frac{w - w_c}{w_o}\right)^{-n} \frac{dT}{d\theta} \tag{21}$$

The logarithm of Eq. (21) is

$$\log k_o - \left(\frac{E}{RT}\right) \log e = \log\left[- \frac{d(w/w_o)}{dT} \left(\frac{w - w_c}{w_o}\right)^{-n} \frac{dT}{d\theta}\right] \tag{22}$$

A plot of the right side of Eq. (22) versus 1/T gives $-(E/R) \log e$ as the slope and $\log k_o$ as the intercept when E, k_o, and n are constant. In order to plot Eq. (22), the value of the reaction order n must be known. Methods 1 and 2 can be used to determine this parameter, since the reaction order is given by the intercept of the plot determined by Eq. (17) and as the slope of the plot determined by Eq. (20). Method 1 also gives the activation energy of the reaction. Unfortunately, it is difficult to accurately determine the slope of Eq. (17) from these data as noted in Fig. 9. Therefore, the procedure used to calculate the kinetic coefficients for each reaction was to determine the best whole-number value of the reaction order from plots of Eqs. (17) and (20), and then to use this reaction order to plot the Arrhenius equation. The activation energy determined from the Arrhenius equation was then used to form a new plot of Eq. (17). Figures 9 and 11 show the results.

A reaction order of 3 is indicated by both methods 1 and 2 for phenolic reaction I. Figures 9 and 11 show that, by using this order, both methods 1 and 3 give a consistent

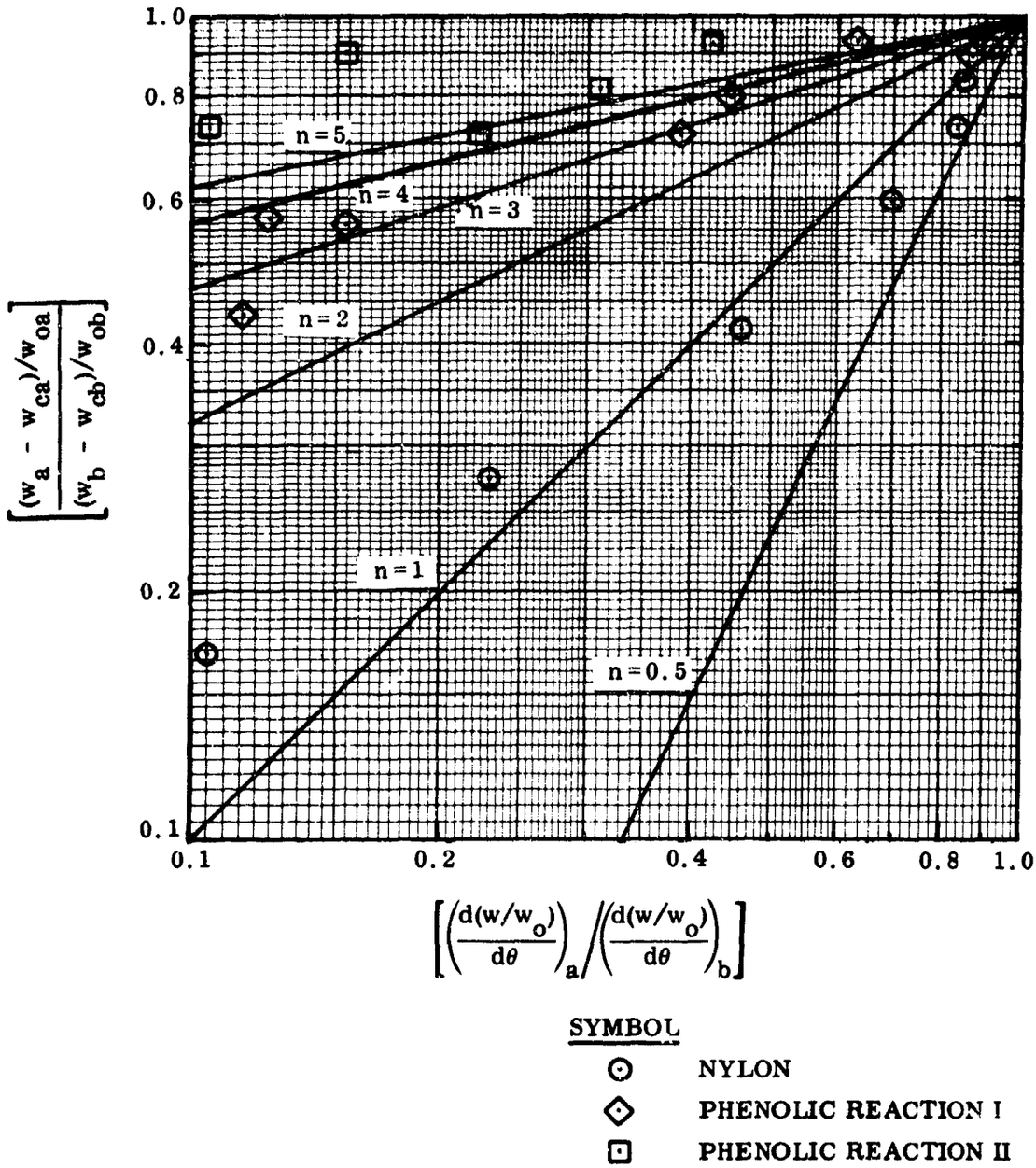

Fig. 10 Rate Equation Ratio Plot, Eq. (20), Used to Determine Reaction Order

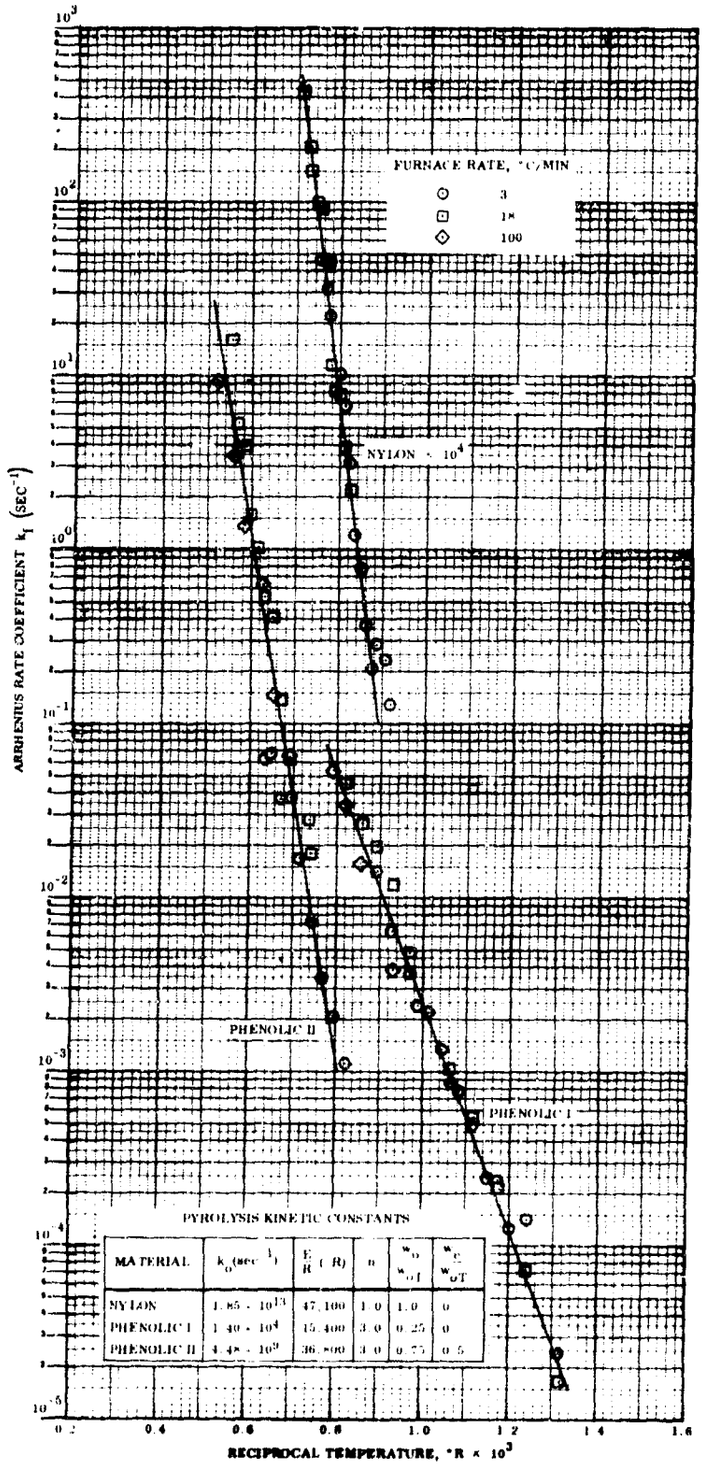

PYROLYSIS KINETIC CONSTANTS

MATERIAL	k_0 (sec⁻¹)	$\frac{E}{R}$ (°R)	n	$\frac{w_0}{w_{0I}}$	$\frac{w_c}{w_{0T}}$
NYLON	1.85×10^{13}	47,100	1.0	1.0	0
PHENOLIC I	1.40×10^{4}	15,400	3.0	0.25	0
PHENOLIC II	4.48×10^{9}	36,800	3.0	0.75	0.5

Fig. 11 Arrhenius Correlation of TGA Rate Data

value of the activation energy, namely 30,600 Btu/lb-mole. The specific rate constant k_o from Fig. 11 is 1.40×10^4 sec^{-1}. An important point to note is that the Arrhenius plot is a straight line and there is no regular deviation from linearity in the temperature range shown. If an incorrect reaction order had been chosen, different rate coefficients would be determined from TGA data for each rate of temperature rise. The fact that the data fit a single straight-line Arrhenius plot for the nearly two orders-of-magnitude range in rates of temperature rise indicates that the analysis is essentially valid.

The reaction order indicated for reaction II by Method 1 was 3, and by Method 2 was greater than 5. Using a reaction order of 3, a linear Arrhenius plot is derived in Fig. 11. The higher value of the reaction order determined by Method 2 was not used because a higher order would not give better correlation between experimental data and theoretical equations. Additionally, the use of this higher order would be difficult to justify on theoretical grounds. As Figs. 8 and 10 show, the activation energy and specific rate constant are 73,200 Btu/lb-mole and 4.48×10^9/sec respectively. The fact that a straight-line Arrhenius plot is derived from TGA covering a nearly two orders-of-magnitude range in rates of temperature rise again indicates the validity of the analysis.

The pyrolysis kinetics of nylon were analyzed in essentially the same manner as for phenolic. Since only one maximum occurs in the rate-of-weight-loss-versus-temperature plot (Fig. 9), only one reaction is assumed to take place. Further, the char weight w_c in Eq. (5) is assumed to be zero. The rate equation then takes the form

$$\left[\frac{d\,(w/w_o)}{d\theta}\right]_N = -\,k_{oN} e^{-E_N/RT} \left(\frac{w}{w_o}\right)^n \tag{23}$$

Using the data from Figs. 4 and 5, Eqs. (17), (20), and (22) may be evaluated to determine the kinetic coefficients for nylon. Figures 9 and 10 show that the reaction order

for nylon is 1. Figures 9 and 11 show that the value of the activation energy and specific rate constant are 94,800 Btu/lb-mole and 1.85×10^{13}/sec respectively. Good correlation of the data obtained by all three methods indicates that the kinetic coefficients are valid.

Section 4
CORRELATION OF EXPERIMENTAL DATA AND THEORY

The equations derived in the previous section should now fit the data from which they were derived. In order to calculate TGA curves from the theoretical equations the integrals of these equations must be determined. Equation (7) may be rearranged as

$$\frac{d\,(w/w_o)}{[(w - w_c)/w_o]^n} = -\frac{k_o}{c} e^{-E/RT}\, dT \tag{24}$$

The left side of Eq. (24) may be integrated by standard methods. For $n = 1$

$$\int_{w_o/w_1}^{w/w_o} \frac{d\,(w/w_o)}{[(w - w_c)/w_o]^n} = \ln\left[\frac{(w - w_c)/w_o}{(w_o - w_c)/w_o}\right] \tag{25}$$

and for $n \neq 1$

$$\int_{w_o/w_1}^{w/w_o} \frac{d\,(w/w_o)}{[(w - w_c)/w_o]^n} = \frac{1}{1-n}\left[\left(\frac{w - w_c}{w_o}\right)^{1-n} - \left(\frac{w_o - w_c}{w_o}\right)^{1-n}\right]^{1/1-n} \tag{26}$$

The integration of the right side of Eq. (24) with respect to temperature is somewhat more complicated. Let

$$X = -\frac{E}{RT}; \qquad \mu = \frac{T}{T_a}; \qquad d\mu = \frac{dT}{T_a} \tag{27}$$

where T_a is upper limit of integration. Then

$$-\frac{k_o}{C}\int_o^{T_a} e^{-E/RT}\,dT = \frac{-k_o T_a}{C}\int_o^1 e^{-X/\mu}\,d\mu \tag{28}$$

The term $\int_o^1 e^{-X/\mu}\,d\mu$ was calculated for values of X varying from 0 to 10 in Ref. 5. The appendix lists values of this integral for X between 10 and 50.

Equation (23) may now be integrated, using Eqs. (26) and (28) to describe the weight loss of nylon as a function of temperature for a constant rate of temperature rise:

$$\frac{w}{w_o} = 10^{-\left[(k_o/C)\,T_a\int_o^1 e^{-X/\mu}\,d\mu\right]} \tag{29}$$

Similarly, Eq. (9) may be integrated, using Eqs. (25) and (28), to predict the weight loss of phenolic:

$$\left(\frac{w}{w_o}\right) = \left[\frac{(n_I - 1)\,k_{oI}T_a\int_o^1 e^{-X/\mu}\,d\mu}{C} + \left(\frac{w_{oI} - w_{cI}}{w_{oI}}\right)^{1-n_I}\right]^{1/1-n_I} + \left(\frac{w_{cI} + w_{cII}}{w_o}\right)$$

$$+ \left[\frac{(n_{II} - 1)\,k_{oII}T_a\int_o^1 e^{-X/\mu}\,d\mu}{C} + \left(\frac{w_{oII} - w_{cII}}{w_{oII}}\right)^{1-n_{II}}\right]^{1/1-n_{II}} \tag{30}$$

Figures 12 and 13 show these equations plotted against experimental data.

The correlation between the phenolic data and Eq. (30) shown in Fig. 12 illustrates the advantages of assuming a two-step depolymerization. Only the two-step process can account for both the early and latter part of the degradation process. Previous analyses have treated either the early degradation period (Ref. 3) or the latter degradation period (Ref. 1), but not both. Friedman (Ref. 1) pointed out that both periods had to be treated to completely describe pyrolysis. Using the two-step method, Eq. (30) is able to predict the entire pyrolysis process within the limits of experimental accuracy. Of particular note is the correspondence between the theory and data for the weight-versus-temperature plots between 1100°R and 1600°R. No previous analysis has achieved similar success in this region. It is also noteworthy that the theory fits TGA data for nearly a two orders-of-magnitude variation in rate of temperature rise, a much larger range than has been attempted in earlier analyses.

Correlation between the theory for nylon, Eq. (29), and TGA data is quite satisfactory as noted in Fig. 13. The fit is excellent throughout nearly the complete pyrolysis range. However, the data show a 4 percent char while theory predicts no char. This difference is a consequence of the assumption that no appreciable char remained at the end of pyrolysis. This assumption was made to simplify the analysis since, for all practical purposes, the 4 percent char retained is unimportant. The correlation shows that a one-step kinetic process is sufficient to describe the pyrolysis data for nylon. This is consistent with earlier analyses (Ref. 2).

Figure 12 also shows data obtained by Doyle (Ref. 6) for nylon,plotted against Eq. (29). The good agreement demonstrated indicates that the analysis for nylon 6-6 is generally valid.

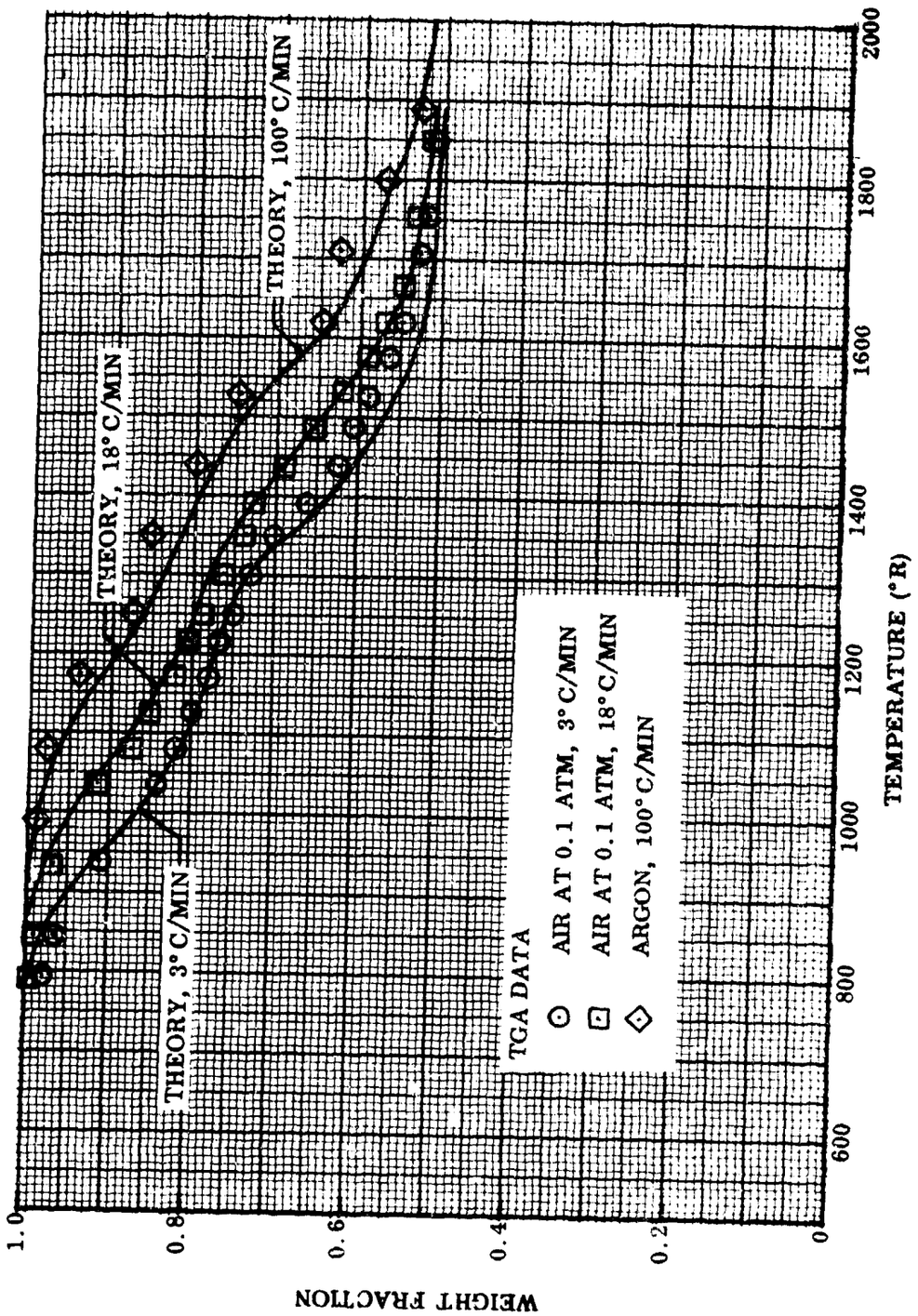

Fig. 12 Comparison of Theory and TGA Rate Data – Phenolic 91LD Resin

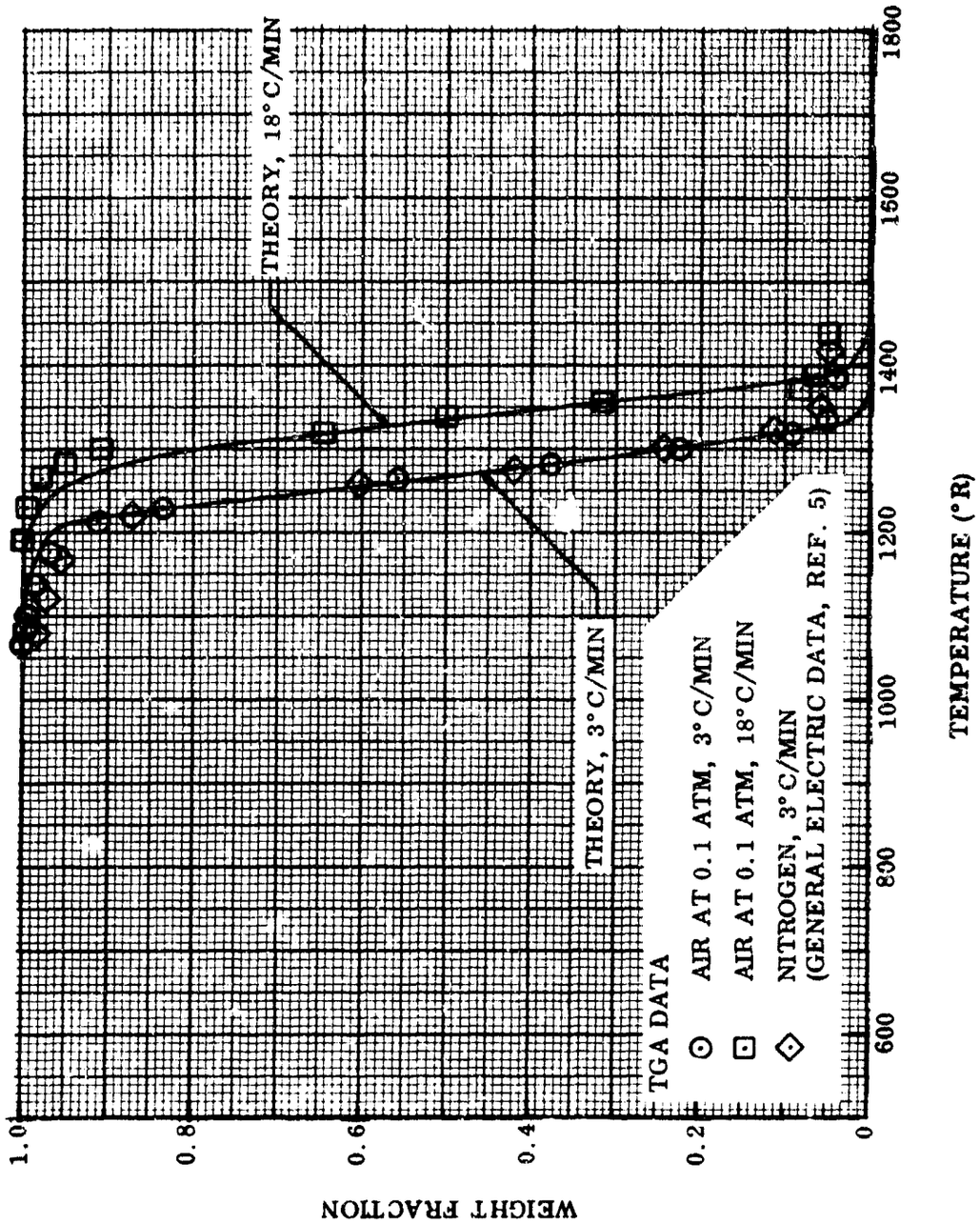

Fig. 13 Comparison of Theory and TGA Rate Data – Nylon 6-6 Fabric

It the assumption that the pyrolysis kinetics of nylon and phenolic are independent of each other is correct for the composite, the kinetics of a composite of nylon and phenolic should be described as the sum of Eqs. (9) and (23):

$$\left(\frac{d\, w/w_o}{d\theta}\right)_{comp.} = \Gamma\left(\frac{d\, w/w_o}{d\theta}\right)_P + (1 - \Gamma)\left(\frac{d\, w/w_o}{d\theta}\right)_N \tag{31}$$

Integration of Eq. (31) with respect to time gives

$$\left(\frac{w}{w_o}\right)_{comp.} = \Gamma\left\{\left[(n_I - 1)\, k_{oI}\, 10^{-E_I/2.3\,RT}\,\theta + \left(\frac{w_{oI} - w_{cI}}{w_{oI}}\right)^{1-n_I}\right]^{1/1-n_I}\right.$$

$$+ \left[(n_{II} - 1)\, k_{oII} 10^{-E_{II}/RT}\,\theta + \left(\frac{w_{oII} - w_{cII}}{w_{oII}}\right)^{1-n_{II}}\right]^{1/1-n_{II}}$$

$$\left. + \left(\frac{w_{cI} + w_{cII}}{w_{oI} + w_{oII}}\right)\right\} + (1 - \Gamma)\, 10^{-\left[\frac{k_{oN}\, e^{-E_N/RT}\,\theta}{2.3}\right]} \tag{32}$$

For a 1:1 weight ratio composite of nylon and phenolic, $\Gamma = 0.50$.

This equation should predict the weight-pyrolyzed-versus-time data for isothermal degradation of a 1:1 composite. Figure 14 shows a comparison of isothermal pyrolysis data and the predicted results. This correlation is a severe test of the theoretical equations. First, the data were not used in any way in the derivation of the equations. Second, these data are for isothermal pyrolysis while the equations were derived from nonisothermal pyrolysis data. Predictions are within 5 percent of the experimentally determined degradation in all cases, indicating the validity of the individual equations and of the assumption that the pyrolysis kinetics of the components are independent of

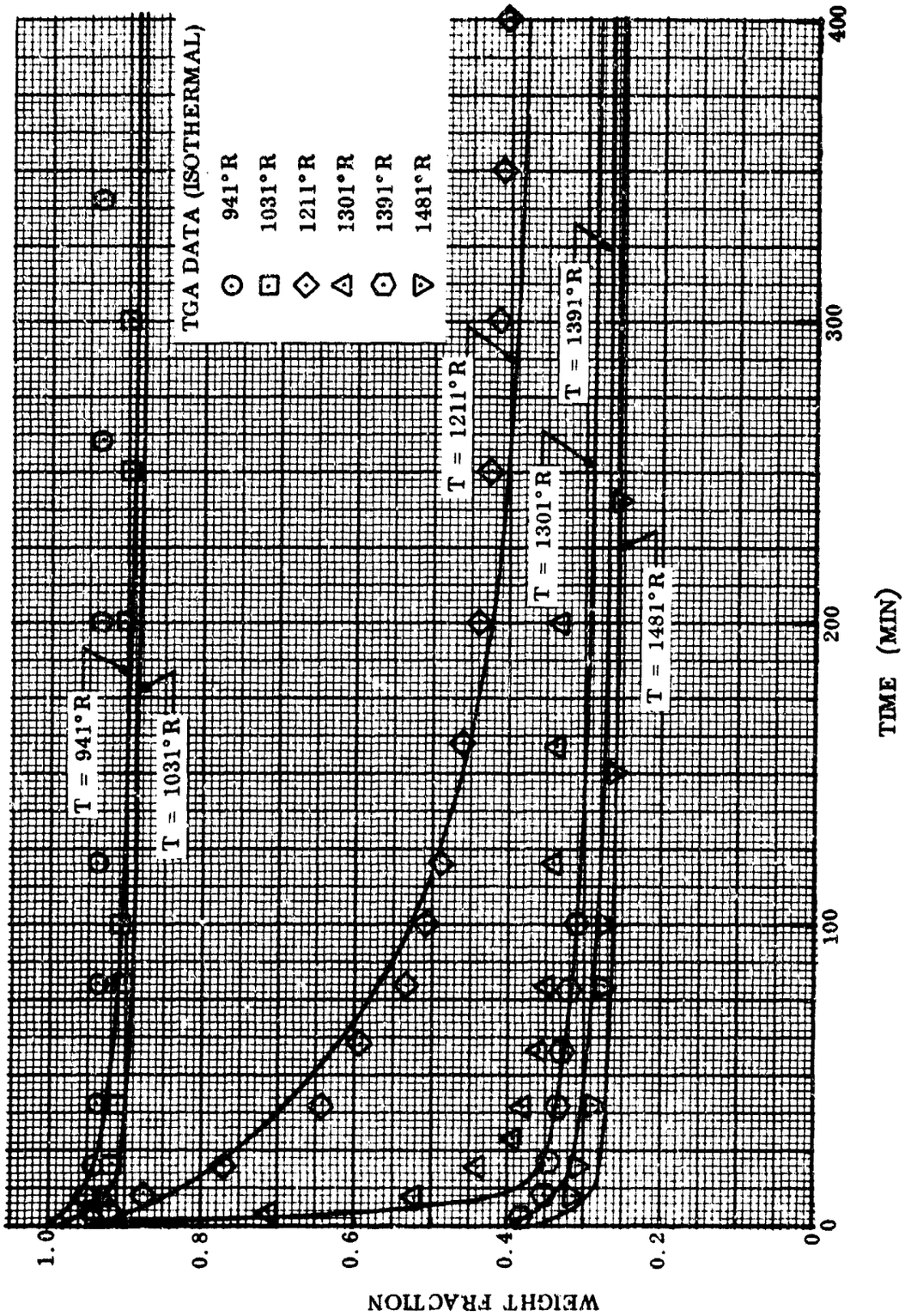

Fig. 14 Comparison of Theory and TGA Rate Data – 1:1 Resin-Fabric Weight Ratio Composite

each other in the composite. Of particular interest is the fact that these equations predict very closely the pyrolysis at 941 and 1031°R and yet also predict very accurately the pyrolysis at 1211°R. If a two-step reaction for phenolic is not used, the initial pyrolysis at the low temperatures cannot easily be accounted for.

When Eq. (31) is integrated with respect to temperature for $dT/d\theta = C$,

$$\left(\frac{w}{w_o}\right)_{comp.} = \Gamma \left(\frac{w}{w_o}\right)_P + (1 - \Gamma)\left(\frac{w}{w_o}\right)_N \tag{33}$$

Here, $(w/w_o)_N$ and $(w/w_o)_P$ are defined by Eqs. (29) and (30) respectively. Equation (33) should predict the weight-versus-temperature data for a composite degraded at a fixed rate of temperature rise. Figures 15, 16, and 17 show TGA data and theoretical predictions for the composite, at three rates of temperature rise; 3, 18, and 60°C/min. These three plots illustrate changes in the TGA as the rate of temperature rise increases. When the rate of temperature rise is 3°C/min, a definite decrease in the weight-versus-temperature curve occurs between 800°R and 1100°R during which about 10 percent of the total material is pyrolyzed (Fig. 15). This same weight decrease appears to a somewhat lesser extent when rate of temperature rise is 18°C/min starting and ending at higher temperatures (Fig. 16). When the rate of temperature rise is 60°C/min the initial weight decrease nearly disappears (Fig. 17). Without using a multi-step kinetic process this phenomena cannot be described mathematically. Using the sum of the two-step phenolic equation and one-step nylon equation, one sees that this shift in initial weight loss is primarily due to the low activation energy of the first phenolic reaction. As the rate of temperature rise increases, the temperature at which phenolic reaction I takes place shifts much more quickly to higher temperature than either the nylon or the second phenolic reaction. As this shift occurs, the first phenolic reaction is superimposed on the second phenolic and nylon reactions and is therefore no longer visible as a separate step in the TGA. The comparison described above illustrates the good correlation that can be obtained between TGA data and the multi-step pyrolysis theory.

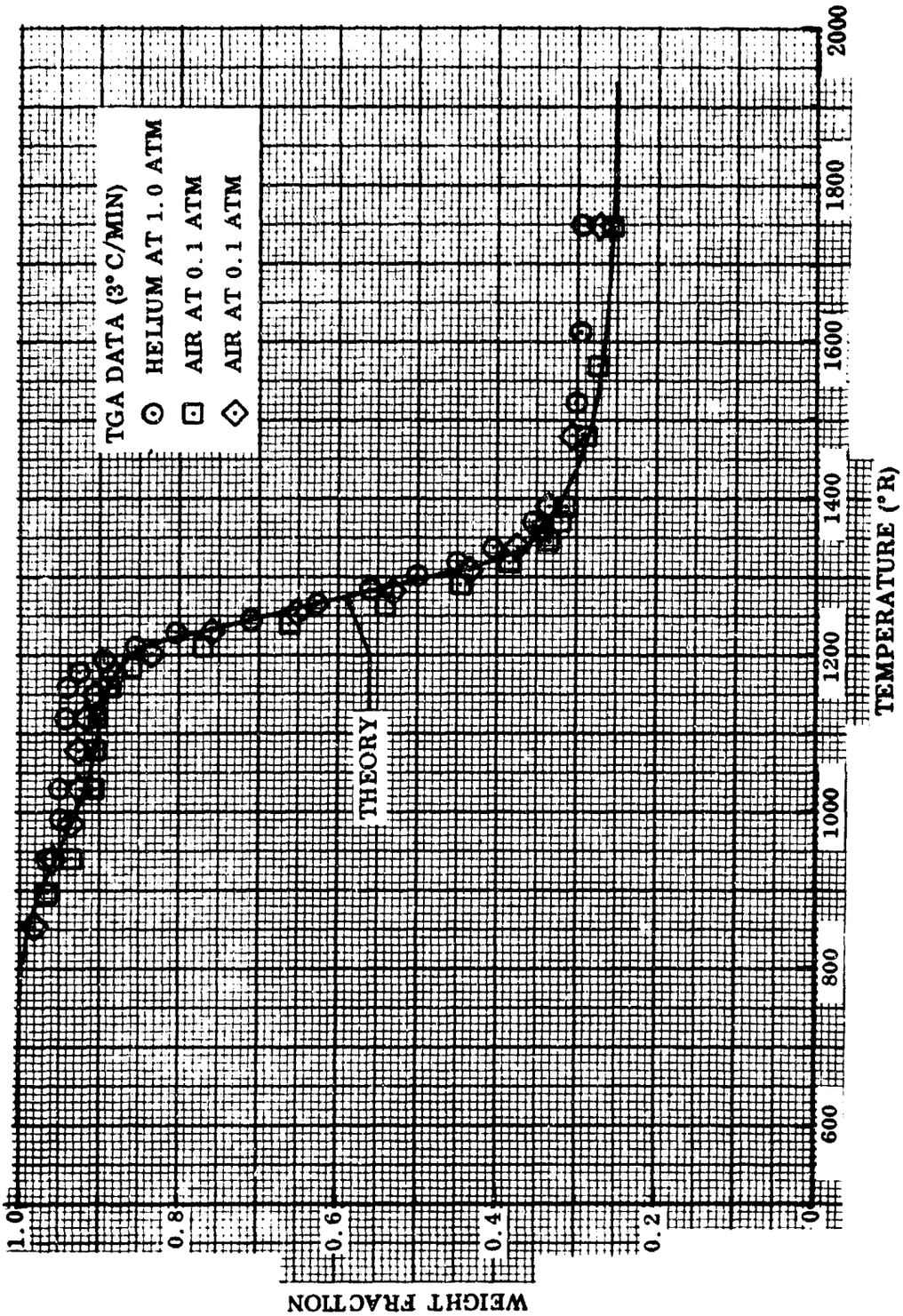

Fig. 15 Comparison of Theory and TGA Rate Data – 1:1 Resin-Fabric Weight Ratio Composite

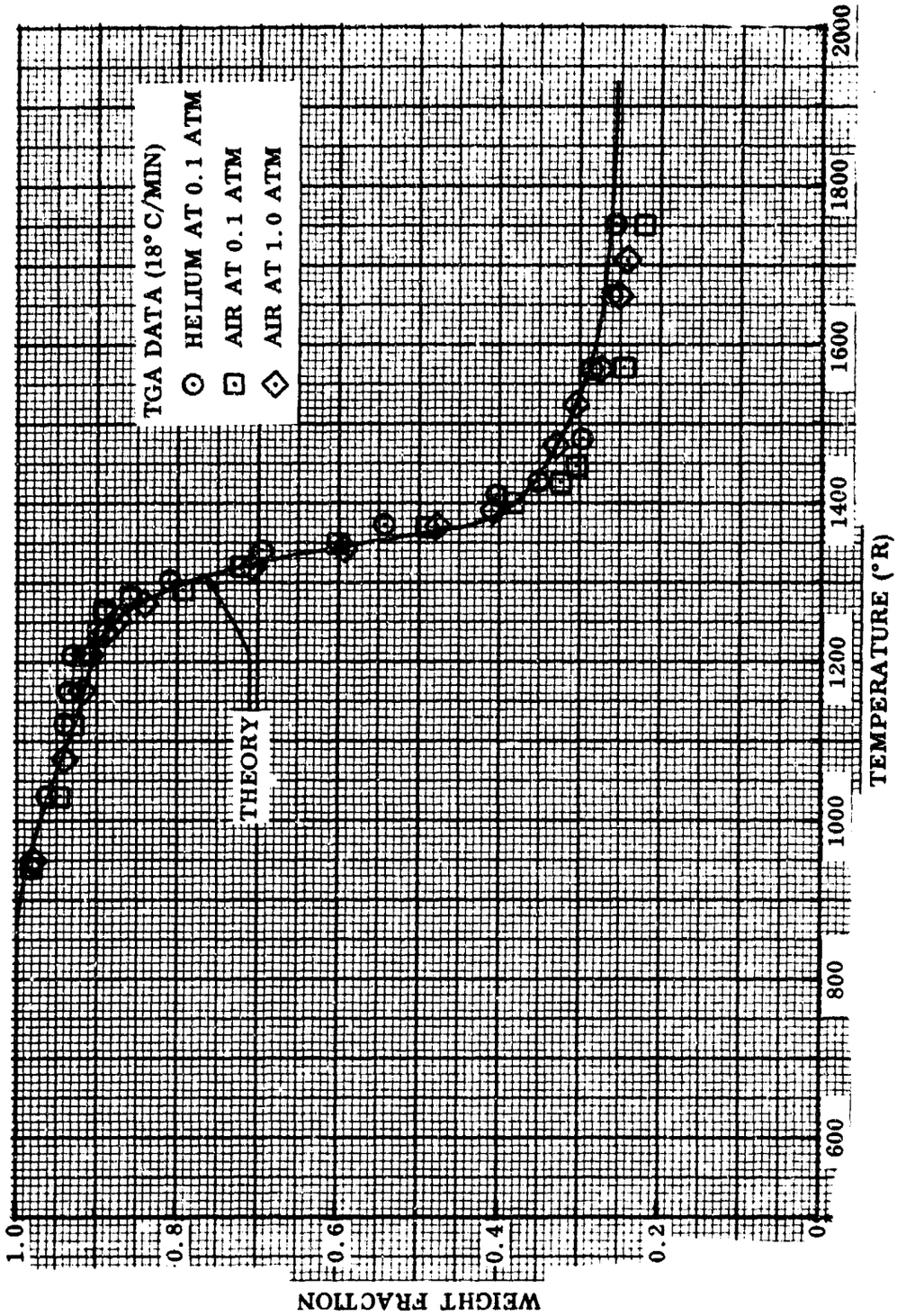

Fig. 16 Comparison of Theory and TGA Rate Data – 1:1 Resin-Fabric Weight Ratio Composite

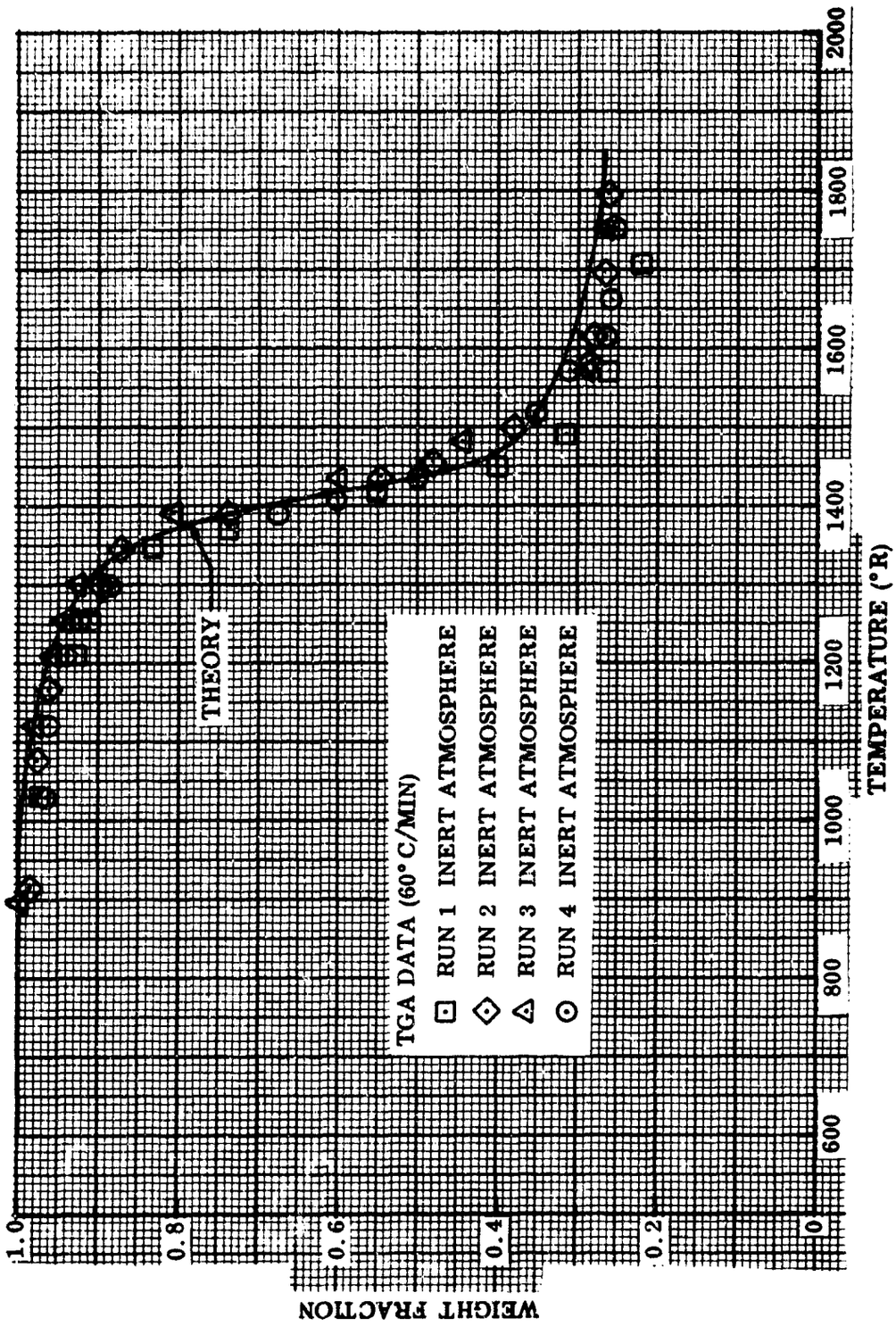

Fig. 17 Comparison of Theory and TGA Rate Data – 1:1 Resin-Fabric Weight Ratio Composite

One very important advantage of the multi-step theory over the single-step theory is its versatility. When a single-step kinetic theory is used, every time the weight fractions of components are changed new kinetic constants must be derived. Using the multi-step theory one simply changes the value of Γ to account for a change in weight fraction. The following paragraph illustrates how useful this can be.

Figure 18 compares the theoretical equations with TGA data for a material obtained from a satellite-vehicle entry heat shield. The nylon-phenolic material (produced by General Electric) is supposed to be similar in weight ratio to the material in the present study. However, TGA data indicate that only 20 percent char remains after pyrolysis of the heat-shield material. Elemental analysis indicates that the material is richer in hydrogen than the 1:1 composite studied herein. Both of these pieces of information would infer that the material has a higher ratio of nylon to phenolic than 1:1. Since no appreciable char is left after pyrolysis of nylon, all the char remaining after pyrolysis of this composite must be due to phenolic. Since the phenolic yields 50 percent char when pyrolyzed, the satellite heat-shield material must be a 6:4 weight-ratio composite of nylon and phenolic if the components are the same as those considered in this analysis.

In Fig. 18 the theory for both a 1:1 mass ratio and a 6:4 mass ratio of nylon to phenolic is shown. As the figure illustrates, the 6:4 weight ratio theory fits these data quite well, particularly in the low-temperature region.

Doyle (Ref. 7) published a TGA for the General Electric nylon-phenolic composite material. His data are shown in Fig. 19. These data again show only 20 percent char. No weight ratios of nylon to phenolic were published with the data, but similarity between TGAs of the satellite vehicle material and Doyle's TGA indicates that they are of the same material. A comparison of Doyle's data and the 6:4 weight-ratio theory indicates good agreement. The fit is particularly good for the early degradation, once again supporting the multi-step pyrolysis theory.

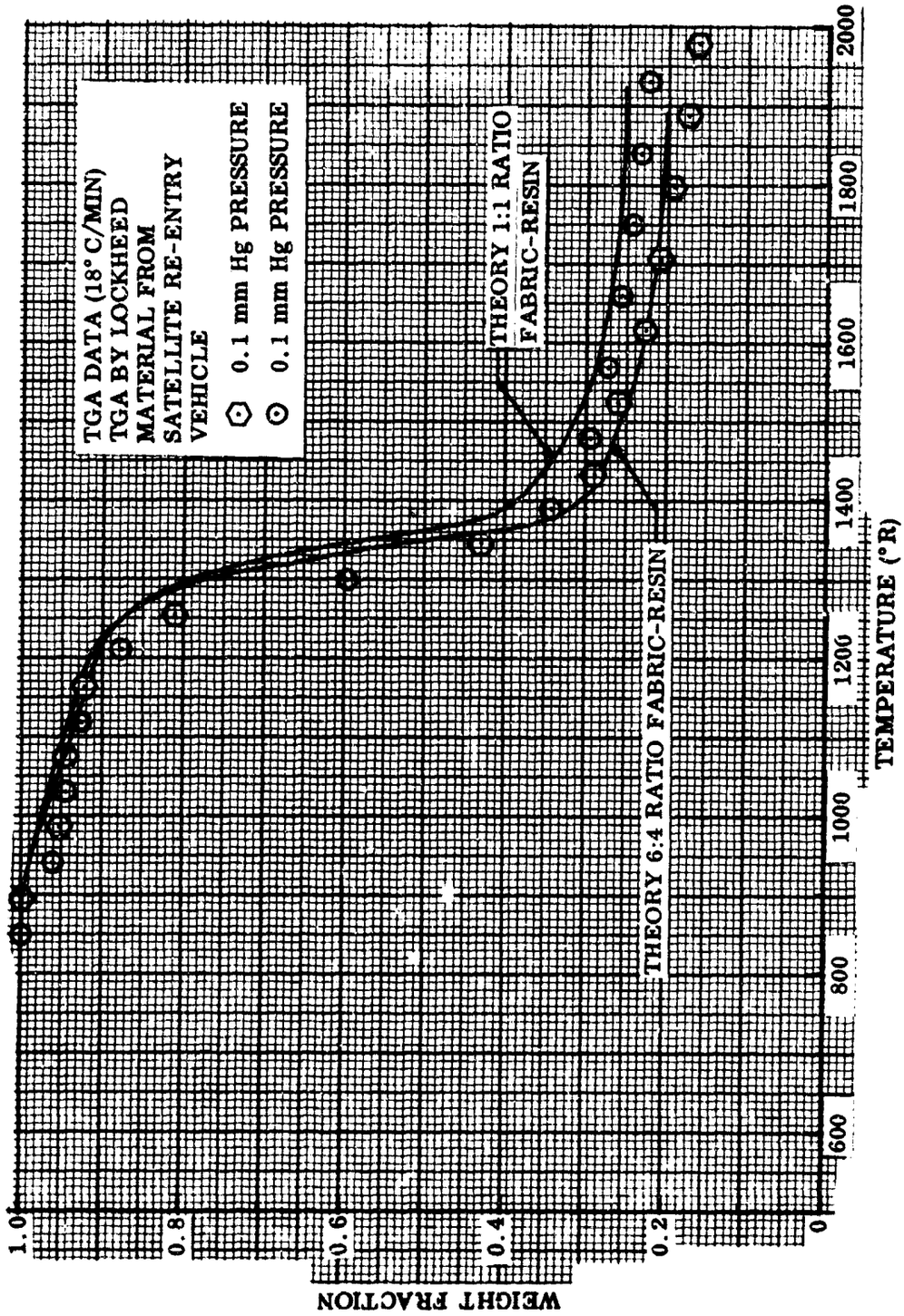

Fig. 18 Comparison of Theory and TGA Rate Data – General Electric Nylon-Phenolic

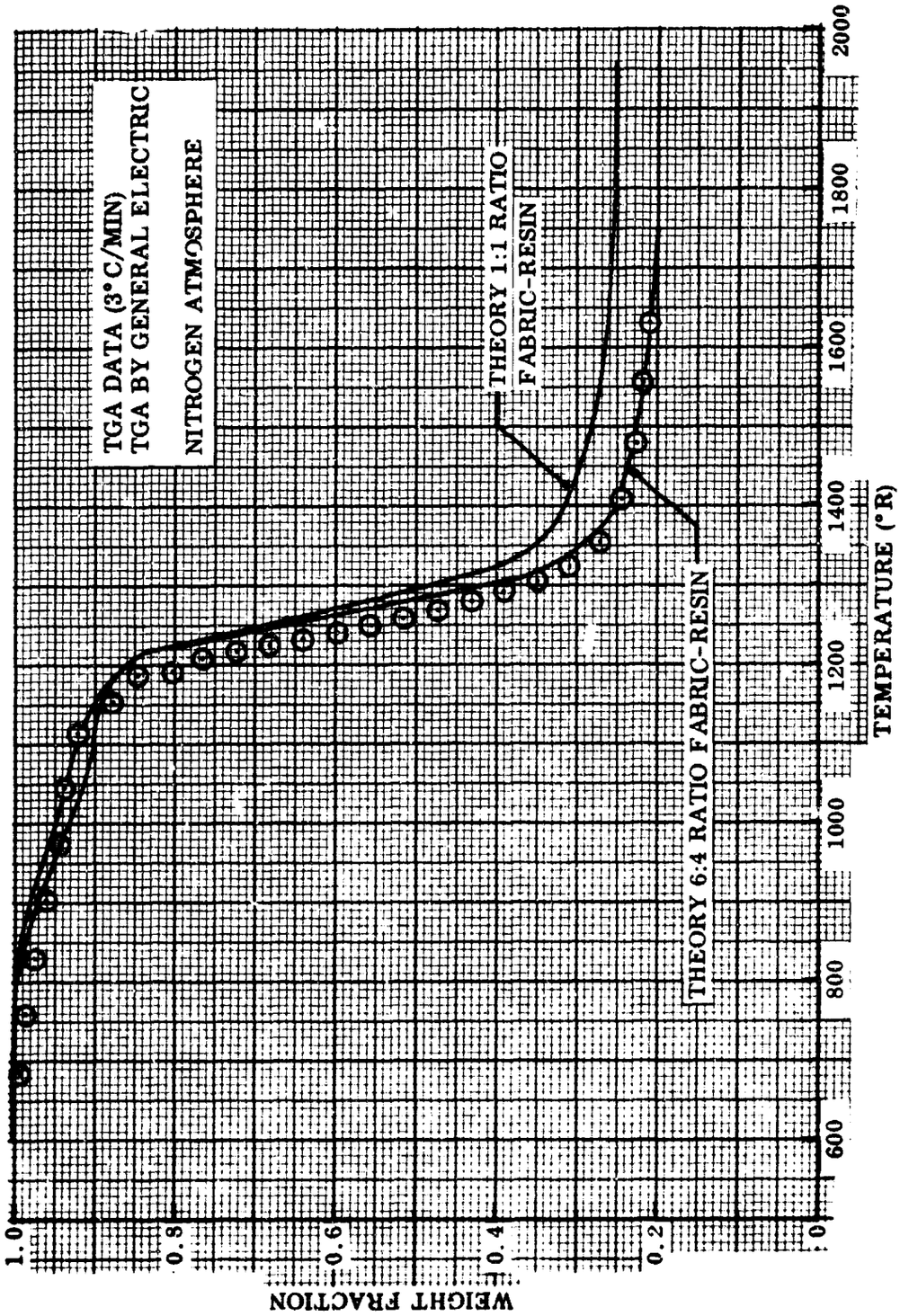

Fig. 19 Comparison of Theory and TGA Rate Data – General Electric Nylon-Phenolic

Section 5
CONCLUSIONS

Agreement between TGA data for the composite and rate equations derived from nylon TGAs and phenolic TGAs individually indicates that the method of analysis is essentially valid. The ability of the rate equations to predict a large range of data from several investigations demonstrates their versatility.

Section 6
REFERENCES

1. H. L. Friedman, "The Kinetics of Thermal Degradation of Charring Plastics, 1. Glass Reinforced Phenolformaldehyde," General Electric Space Sciences Laboratory, Doc. No. R61SD145, August 1961
2. S. Straus and L. A. Wall, "Pyrolysis of Polyamides," Journal of Research, National Bureau of Standards, Vol. 60, 1958, p. 39
3. S. L. Madorsky and S. Straus, "Thermal Degradation of Polymers at Temperatures up to 1200° C," WADC TR 59-64, Part II, April 1960
4. M. Honma, R. J. Grassi, E. Kowasaki, and R. J. Wethern, "Thermal Degradation of Polymeric Materials," LMSC Materials Sciences Laboratory, 16 December 1963
5. E. S. Freeman and B. Carrol, "The Application of Thermoanalytical Technique to Reaction Kinetics. The Thermogravimetric Evaluation of the Kinetics of Decomposition of Calcium Oxalate Monohydrate," Journal of Phys. Chem., Vol. 662, 1958, pp. 394–397
6. K. M. Case, et al, "Introduction to the Theory of Neutron Diffraction," U.S. Government Printing Office, 1953
7. C. D. Doyle, "Evaluation of Experimental Polymers," WADD TR 60-283, June 1960

Appendix
THE EXPONENTIAL INTEGRAL $E_2(X)$

The exponential integral $E_2(X)$ defined by

$$E_2(X) = \int_0^\infty e^{-\mu X} \mu^{-2} \, d\mu = \int_0^1 e^{X/\mu} \, d\mu \qquad (A.1)$$

occurs often enough in thermodynamics, particularly in reaction kinetics, to make a tabulation useful. Reference 6 tabulates this function for values of X between 0 and 10. However, many applications require a much greater range. For this reason, a short computer program in the FORTRAN IV language was written to extend the tabulation from $X = 10$ to $X = 50$.

Simpson's composite formula was applied to the right-hand side of Eq. (A.1) for each value of X considered. Since the error in approximation increases with increasing X, two separate calculations were made. For $10 \leq X \leq 35$, the interval $0 \leq \mu \leq 1$ was divided into 5000 increments. In both cases, doubling the number of increments at a few points was found to affect only the fifth and following significant digits, so the tabulated values are accurate to four significant figures.

A second possible source of error was also considered. In applying Simpson's rule it was necessary to calculate the function

$$f(\mu) = e^{X/\mu} \qquad (A.2)$$

For $X/\mu > 87.5$, $f(\mu)$ becomes smaller than 10^{-37}, the smallest number representable in the 7094 computer. At such points, therefore, $f(\mu)$ was set arbitrarily to zero. This amounts to neglecting small terms in Simpson's formula, and the resulting error

becomes proportionately greater as X increases. For X = 50 (the largest value tabulated) the error was conservatively estimated to be ten orders-of-magnitude smaller than the value of the integral at that point, indicating that this error may be ignored over the entire range.

Results of the computation are tabulated in Table A-1.

Table A-1

THE EXPONENTIAL INTEGRAL

X	$E_2(X)$	X	$E_2(X)$	X	$E_2(X)$
10.0	3.8299E-06			16.0	6.2866E-09
10.1	3.4361E-06	13.1	1.3651E-07	16.1	5.6566E-09
10.2	3.0831E-06	13.2	1.2269E-07	16.2	5.0898E-09
10.3	2.7665E-06	13.3	1.1028E-07	16.3	4.5800E-09
10.4	2.4826E-06	13.4	9.9129E-08	16.4	4.1214E-09
10.5	2.2280E-06	13.5	8.9108E-08	16.5	3.7089E-09
10.6	1.9996E-06	13.6	8.0104E-08	16.6	3.3377E-09
10.7	1.7948E-06	13.7	7.2013E-08	16.7	3.0037E-09
10.8	1.6110E-06	13.8	6.4742E-08	16.8	2.7033E-09
10.9	1.4462E-06	13.9	5.8207E-08	16.9	2.4330E-09
11.0	1.2983E-06	14.0	5.2334E-08	17.0	2.1897E-09
11.1	1.1656E-06	14.1	4.7056E-08	17.1	1.9709E-09
11.2	1.0465E-06	14.2	4.2312E-08	17.2	1.7739E-09
11.3	9.3967E-07	14.3	3.8047E-08	17.3	1.5967E-09
11.4	8.4378E-07	14.4	3.4214E-08	17.4	1.4373E-09
11.5	7.5772E-07	14.5	3.0768E-08	17.5	1.2938E-09
11.6	6.8048E-07	14.6	2.7670E-08	17.6	1.1646E-09
11.7	6.1114E-07	14.7	2.4885E-08	17.7	1.0484E-09
11.8	5.4890E-07	14.8	2.2381E-08	17.8	9.4379E-10
11.9	4.9303E-07	14.9	2.0130E-08	17.9	8.4964E-10
12.0	4.4287E-07	15.0	1.8106E-08	18.0	7.6491E-10
12.1	3.9783E-07	15.1	1.6286E-08	18.1	6.8864E-10
12.2	3.5740E-07	15.2	1.4649E-08	18.2	6.2000E-10
12.3	3.2109E-07	15.3	1.3178E-08	18.3	5.5821E-10
12.4	2.8848E-07	15.4	1.1854E-08	18.4	5.0259E-10
12.5	2.5920E-07	15.5	1.0664E-08	18.5	4.5253E-10
12.6	2.3290E-07	15.6	9.5941E-09	18.6	4.0746E-10
12.7	2.0928E-07	15.7	8.6315E-09	18.7	3.6689E-10
12.8	1.8806E-07	15.8	7.7657E-09	18.8	3.3036E-10
12.9	1.6901E-07	15.9	6.9870E-09	18.9	2.9748E-10
13.0	1.5189E-07			19.0	2.6788E-10

Table A-1 (cont.)

X	$E_2(X)$	X	$E_2(X)$	X	$E_2(X)$
19.1	2.4123E-10	23.4	2.7155E-12	27.7	3.1486E-14
19.2	2.1724E-10	23.5	2.4474E-12	27.8	2.8394E-14
19.3	1.9563E-10	23.6	2.2058E-12	27.9	2.5606E-14
19.4	1.7618E-10	23.7	1.9881E-12	28.0	2.3091E-14
19.5	1.5867E-10	23.8	1.7919E-12	28.1	2.0824E-14
19.6	1.4290E-10	23.9	1.6151E-12	28.2	1.8780E-14
19.7	1.2870E-10	24.0	1.4557E-12	28.3	1.6936E-14
19.8	1.1592E-10	24.1	1.3121E-12	28.4	1.5274E-14
19.9	1.0440E-10	24.2	1.1827E-12	28.5	1.3775E-14
20.0	9.4034E-11	24.3	1.0661E-12	28.6	1.2423E-14
20.1	8.4698E-11	24.4	9.6094E-13	28.7	1.1204E-14
20.2	7.6290E-11	24.5	8.6620E-13	28.8	1.0105E-14
20.3	6.8718E-11	24.6	7.8081E-13	28.9	9.1137E-15
20.4	6.1899E-11	24.7	7.0384E-13	29.0	8.2197E-15
20.5	5.5758E-11	24.8	6.3447E-13	29.1	7.4135E-15
20.6	5.0227E-11	24.9	5.7195E-13	29.2	6.6864E-15
20.7	4.5245E-11	25.0	5.1560E-13	29.3	6.0307E-15
20.8	4.0759E-11	25.1	4.6480E-13	29.4	5.4394E-15
20.9	3.6718E-11	25.2	4.1901E-13	29.5	4.9061E-15
21.0	3.3078E-11	25.3	3.7774E-13	29.6	4.4251E-15
21.1	2.9800E-11	25.4	3.4054E-13	29.7	3.9913E-15
21.2	2.6847E-11	25.5	3.0701E-13	29.8	3.6001E-15
21.3	2.4187E-11	25.6	2.7678E-13	29.9	3.2472E-15
21.4	2.1791E-11	25.7	2.4953E-13	30.0	2.9280E-15
21.5	1.9633E-11	25.8	2.2497E-13	30.1	2.6420E-15
21.6	1.7689E-11	25.9	2.0283E-13	30.2	2.3831E-15
21.7	1.5938E-11	26.0	1.8287E-13	30.3	2.1496E-15
21.8	1.4360E-11	26.1	1.6488E-13	30.4	1.9390E-15
21	1.2939E-11	26.2	1.4865E-13	30.5	1.7491E-15
22.0	1.1658E-11	26.3	1.3403E-13	30.6	1.5778E-15
22.1	1.0505E-11	26.4	1.2085E-13	30.7	1.4232E-15
22.2	9.4658E-[illegible]	26.5	1.0896E-13	30.8	1.2839E-15
22.3	[illegible]	26.6	9.8245E-14	30.9	1.1581E-15
22.4	[illegible]12	26.7	8.8585E-14	31.0	1.0447E-15
22.5	6.9250E-12	26.8	7.9875E-14	31.1	9.4246E-16
22.6	6.2413E-12	26.9	7.2023E-14	31.2	8.5020E-16
22.7	[illegible].6243E-12	27.0	6.4943E-14	31.3	7.6697E-16
22.8	5.0685E-12	27.1	5.8560E-14	31.4	6.9190E-16
22.9	4.5676E-12	27.2	5.2805E-14	31.5	6.2418E-16
23.0	4.1163E-12	27.3	4.7616E-14	31.6	5.6309E-16
23.1	3.7097E-12	27.4	4.2938E-14	31.7	5.0799E-16
23.2	3.3432E-12	27.5	3.8720E-14	31.8	4.5829E-16
23.3	3.0131E-12	27.6	3.4916E-14	31.9	4.1345E-16

Table A-1 (cont.)

X	$E_2(X)$	X	$E_2(X)$	X	$E_2(X)$
32.0	3.7300E-16	36.4	4.0526E-18	40.8	4.4628E-20
32.1	3.3651E-16	36.5	3.6574E-18	40.9	4.0286E-20
32.2	3.0359E-16	36.6	3.3008E-18	41.0	3.6368E-20
32.3	2.7390E-16	36.7	2.9789E-18	41.1	3.2830E-20
32.4	2.4711E-16	36.8	2.6885E-18	41.2	2.9637E-20
32.5	2.2294E-16	36.9	2.4264E-18	41.3	2.6755E-20
32.6	2.0114E-16	37.0	2.1898E-18	41.4	2.4153E-20
32.7	1.8148E-16	37.1	1.9764E-18	41.5	2.1804E-20
32.8	1.6373E-16	37.2	1.7837E-18	41.6	1.9684E-20
32.9	1.4773E-16	37.3	1.6098E-18	41.7	1.7770E-20
33.0	1.3328E-16	37.4	1.4529E-18	41.8	1.6042E-20
33.1	1.2026E-16	37.5	1.3113E-18	41.9	1.4482E-20
33.2	1.0850E-16	37.6	1.1835E-18	42.0	1.3074E-20
33.3	9.7898E-17	37.7	1.0682E-18	42.1	1.1803E-20
33.4	8.8331E-17	37.8	9.6412E-19	42.2	1.0656E-20
33.5	7.9699E-17	37.9	8.7018E-19	42.3	9.6198E-21
33.6	7.1911E-17	38.0	7.8540E-19	42.4	8.6847E-21
33.7	6.4885E-17	38.1	7.0888E-19	42.5	7.8405E-21
33.8	5.8546E-17	38.2	6.3982E-19	42.6	7.0785E-21
33.9	5.2827E-17	38.3	5.7749E-19	42.7	6.3905E-21
34.0	4.7666E-17	38.4	5.2124E-19	42.8	5.7694E-21
34.1	4.3010E-17	38.5	4.7047E-19	42.9	5.2087E-21
34.2	3.8810E-17	38.6	4.2465E-19	43.0	4.7026E-21
34.3	3.5019E-17	38.7	3.8329E-19	43.1	4.2456E-21
34.4	3.1600E-17	38.8	3.4596E-19	43.2	3.8331E-21
34.5	2.8514E-17	38.9	3.1227E-19	43.3	3.4606E-21
34.6	2.5730E-17	39.0	2.8186E-19	43.4	3.1244E-21
34.7	2.3218E-17	39.1	2.5442E-19	43.5	2.8208E-21
34.8	2.0951E-17	39.2	2.2965E-19	43.6	2.5468E-21
34.9	1.8906E-17	39.3	2.0729E-19	43.7	2.2994E-21
35.0	1.7058E-17	39.4	1.8711E-19	43.8	2.0760E-21
35.1	1.5393E-17	39.5	1.6889E-19	43.9	1.8743E-21
35.2	1.3891E-17	39.6	1.5245E-19	44.0	1.6923E-21
35.3	1.2535E-17	39.7	1.3761E-19	44.1	1.5279E-21
35.4	1.1312E-17	39.8	1.2422E-19	44.2	1.3795E-21
35.5	1.0208E-17	39.9	1.1213E-19	44.3	1.2455E-21
35.6	9.2118E-18	40.0	1.0122E-19	44.4	1.1246E-21
35.7	8.3130E-18	40.1	9.1367E-20	44.5	1.0154E-21
35.8	7.5020E-18	40.2	8.2476E-20	44.6	9.1676E-22
35.9	6.7701E-18	40.3	7.4450E-20	44.7	8.2774E-22
36.0	6.1075E-18	40.4	6.7206E-20	44.8	7.4737E-22
36.1	5.5137E-18	40.5	6.0667E-20	44.9	6.7480E-22
36.2	4.9759E-18	40.6	5.4765E-20	45.0	6.0928E-22
36.3	4.4906E-18	40.7	4.9437E-20	45.1	5.5013E-22

Table A-1 (cont.)

X	$E_2(X)$	X	$E_2(X)$
45.2	4.9672E-22	47.7	3.8718E-23
45.3	4.4850E-22	47.8	3.4963E-23
45.4	4.0496E-22	47.9	3.1572E-23
45.5	3.6565E-22	48.0	2.8511E-23
45.6	3.3016E-22	48.1	2.5746E-23
45.7	2.9811E-22	48.2	2.3249E-23
45.8	2.6918E-22	48.3	2.0995E-23
45.9	2.4305E-22	48.4	1.8959E-23
46.0	2.1946E-22	48.5	1.7121E-23
46.1	1.9816E-22	48.6	1.5461E-23
46.2	1.7893E-22	48.7	1.3962E-23
46.3	1.6157E-22	48.8	1.2608E-23
46.4	1.4589E-22	48.9	1.1386E-23
46.5	1.3174E-22	49.0	1.0282E-23
46.6	1.1895E-22	49.1	9.2857E-24
46.7	1.0741E-22	49.2	3.3856E-24
46.8	9.6991E-23	49.3	7.5728E-24
46.9	8.7581E-23	49.4	6.8388E-24
47.0	7.9085E-23	49.5	6.1759E-24
47.1	7.1413E-23	49.6	5.5774E-24
47.2	6.4485E-23	49.7	5.0368E-24
47.3	5.8230E-23	49.8	4.5487E-24
47.4	5.2582E-23	49.9	4.1079E-24
47.5	4.7482E-23	50.0	3.7098E-24
47.6	4.2876E-23	50.1	3.3503E-24